

Ivar Abas and Hugo Hagedooren

Salt intrusion in the Pungue estuary, Mozambique

A case study on modelling the salinity distribution in the Pungue estuary



Delft, March 2017

Salt intrusion in the Pungue estuary, Mozambique

A case study on modelling the salinity distribution in the Pungue estuary

By
Ivar Abas
and
Hugo Hagedooren

In fulfilment of the requirements of an Additional Master Thesis

Master
Civil Engineering
Track Water Management

at the Delft University of Technology,

Supervisors: Prof. Dr. Ir. H.H.G. Savenije,
Dr. Ir. S.G.J. Heijman,
Ir. W.M.J. Luxemburg

An electronic version of this thesis is available at <http://repository.tudelft.nl/>

Notation

a	Cross-sectional convergence length	[m]
A	Tidal average cross-sectional area	[m ²]
A_0	Cross-sectional area at the estuary mouth	[m ²]
A_r	Cross-sectional area of the river	[m ²]
b	Width convergence length	[m]
B	Tidal average estuary width	[m]
B_0	Width at the estuary mouth	[m]
B_r	Width of the river	[m]
C	Chézy coefficient	[m ^{0.5} /s]
D	Tidal average longitudinal dispersion	[m ² /s]
D_0	Dispersion coefficient at the estuary mouth	[m ² /s]
D_i	Dispersion coefficient during HWS, TA or LWS	[m ² /s]
$D(x)$	Dispersion coefficient as a function of x	[m ² /s]
E	Tidal excursion	[m]
E_0	Tidal excursion at the estuary mouth	[m]
\bar{g}	Gravitational acceleration	[m/s ²]
\bar{h}	Tidal average depth	[m]
h_0	Depth at the estuary mouth	[m]
H	Tidal range	[m]
K	Van der Burgh's coefficient	[-]
L	Salt intrusion length	[m]
P	Wetted perimeter	[m]
P	Tidal prism	[m ³]
P_n	Net rainfall in an estuary	[m/s]
q	Coefficient of the advective term	[m/s]
Q_f	Fresh water discharge	[m ³ /s]
Q_0	Fresh water discharge during dry season	[m ³ /s]
Q_r	River discharge	[m ³ /s]
Q_p	Extraction rate	[m ³ /s]
Q_t	Tidal discharge	[m ³ /s]
r_s	Storage width ratio	[-]
R_S	Source term	[m ² /s]
s	$s(x, t)$ is the salinity	[kg/m ³]
S_f	Fresh water salinity	[kg/m ³]
S_i	Salinity during HWS, TA or LWS condition	[kg/m ³]
$S(x)$	Salinity as a function of x	[kg/m ³]
S_0	Sea salinity	[kg/m ³]
S_{\max_intake}	Salinity threshold of the intake	[kg/m ³]
t	Time	[s]
T	Tidal period	[s]
x	Distance from the estuary mouth	[m]
β	Dispersion reduction rate	[-]
δ	Damping number	[-]
η	Tidal amplitude	[m]
ρ	Density of fresh water	[kg/m ³]
$\Delta\rho$	Density difference between salt and fresh water	[kg/m ³]

Preface

Before reading our research we would like to introduce ourselves. We are Ivar Abas and Hugo Hagedooren, two students of the master Watermanagement at the faculty of Civil Engineering at the Delft University of Technology. This research is conducted to fulfil the requirements of an additional master thesis, which is part of our master programme. This research is done in the period September 2016 until March 2017. In this period there was a field visit of six weeks to Mozambique.

This visit to Mozambique was a very interesting and educational experience. Our stay was not without some practical problems such as: engine failure, getting stuck on a sandbank, hippos blocking our way and malaria. So at the end we are very happy that we were able to conduct enough measurements.

We hope you enjoy reading our additional master thesis.

Acknowledgements

As authors we want to thank everyone who contributed in any way to our research. First of all we want to thank the Mafambisse sugarcane estate (Tongaat Hulett Sugar) for their hospitality during our stay in Mozambique. In particular we want to thank Fungai Nyemba and Alasdair Harris for arranging everything in advance. We also want to thank Fungai Nyemba for arranging pleasant accommodation and helping us out with all the necessary transport. We want to thank Collert Moyo for providing technical information on all kinds of issues we encountered during our research and the answers he gave to all our questions. Special thanks go to Len of the irrigation workshop for building the diver installation cages and for the enjoyable evenings in the restaurant of the estate.

Of course we want to warmly thank our professor Huub Savenije for inspiring us with his knowledge of alluvial estuaries and his corresponding enthusiasm. Our discussions were very fruitful and we enjoyed working together. We also would like to thank Willem Luxemburg for his advice and help with the preparation of our measurement equipment and methods.

We would like to thank Van Essen instruments for providing us with CTD – divers and advise how to use them.

Last but certainly not least we have to thank ARA-Centro and in particular Antonio Melembe, Castro Júnior and Bimbo for all their help. They provided us with a fantastic boat, hydrological data and accompanied us on all our field trips. Even if we had to get up very early in the morning you guys stood ready to help us out. We cannot thank you enough and it is hard to express our appreciation in words. We hope we get the opportunity to meet you guys again and we will remember the special moments.

Special thanks are given to the TBI fund and the Lamminga fund for supporting us financially and making it possible to go on field visit in Mozambique.

Contents

Notation	4
Preface	5
Acknowledgements	5
Abstract.....	8
1. Introduction.....	9
1.1 Estuary description	9
1.2 Problem statement	10
1.3 Research objective	10
2. Theory on salt intrusion	11
2.1 Geometry alluvial estuaries	11
2.2 The tidal wave	12
2.3 Mixing processes in alluvial estuaries	13
2.4 Steady state model	16
2.5 Unsteady state model	17
2.5.1 Theory of unsteady state model	17
2.5.2 Application of unsteady state model	19
3. Description of the study.....	20
3.1 Estuary geometry	20
3.2 River discharge	20
3.3 Salinity measurements	20
4. Elaboration on salt intrusion models	22
4.1 Determination estuary geometry.....	22
4.2 Application steady state model.....	24
4.2.1 Calibration steady state model	24
4.2.2 Irregularities in salinity measurements.....	25
4.3 Application unsteady state model.....	28
4.3.1 Calibration unsteady state model	28
4.3.2 Additional salt source in unsteady state model.....	29
4.3.3 Calculation additional salinity source	30
4.3.4 Virtual experiment alternated pumping.....	31

5. Development of scenarios	32
5.1 Set up of the scenarios	32
5.2 Scenario 0: reference situation	34
5.3 Scenario 1: expansion of the intake of FIPAG	35
5.4 Scenario 2: increased extraction rate of the estate	36
5.5 Scenario 3: a drought	37
5.6 Scenario 4: bend cutoff	38
5.7 Summary of the scenarios	40
6. Conclusions and recommendations	41
6.1 Conclusions	41
6.2 Recommendations.....	42
6.2.1 Relocation of the intake.....	42
6.2.2 Alternated pumping.....	42
6.2.3 Monitoring an additional salt source	43
7. Further research.....	44
References.....	46
List of figures.....	47
List of tables.....	47
Appendix A: determination geometry parameters	48
Appendix B: Gumbel extreme value distribution.....	50
B.1: Gumbel type I.....	50
B.2: Log-Gumbel type III	51

Abstract

The Pungue river originates in Zimbabwe and drains into the Indian Ocean creating a large alluvial estuary. The river discharge generated in the Eastern Highlands of Zimbabwe is an important source of fresh water for water consumers in Mozambique. In Mozambique the fresh water is used for drinking water production for the city of Beira and for irrigation and process purposes of the sugarcane estate of Mafambisse.

The Mafambisse sugarcane estate strongly depends on the fresh water supply of the Pungue river. In the dry season when a low discharge is combined with a high tidal range salt intrusion can lead to high salinity values at the water intake of the estate. If the salinity exceeds the threshold of 0.16 kg/m^3 the water cannot be taken in, without seriously affecting the yield or the operation of the sugarcane factory.

The objective of this research is to obtain a thorough insight in the characteristics of the salt intrusion in the Pungue estuary in order to give preliminary solutions to the sugarcane estate. To get insight in the characteristics of salt intrusion data is collected during November and December of 2016. In order to describe the parameters in the steady and unsteady state salt intrusion models the estuary geometry is determined, the river discharge has been measured and salinity measurements have been conducted.

The steady state salt intrusion model is calibrated on salinity measurements carried out with the moving-boat method. The salinity measurements show a sudden increase in salinity values around 60 kilometres from the estuary mouth. From the calibration it becomes clear that the steady state model is not able to represent these irregularities in the salinity distribution. This research shows that it is likely that an additional source of salt is causing the increase in salinity values and that the unsteady state salt intrusion is able to represent this.

To see the effect of extreme situations of the tide and river discharge on the salinity distribution in the Pungue estuary four scenarios have been developed and compared with a reference scenario. The following scenarios are chosen: expansion of FIPAG (drinking water company), an increased extraction rate of Mafambisse, a drought and a bend cutoff. From the scenarios it can be concluded that with exception of the expansion of FIPAG all scenarios exceed the salinity threshold at the intake causing serious water shortages. The most extreme situation is reached in case of a drought. The salinity value modelled at the intake becomes 2.63 kg/m^3 and the salt intrudes up to 84.5 km. In this situation no extractions are possible and Mafambisse will suffer from severe water shortages.

To provide the sugarcane estate with preliminary solutions in preventing salinity incidents at the intake this research elaborates on three concrete recommendations. A straightforward solution to reduce salt incidents at the intake would be the relocation of the pumping station. This research suggests relocating the pumping station to 90 km or further from the estuary mouth.

Another solution offered would be an alternated pumping scheme. This research shows that alternated pumping can be beneficial under certain conditions; a high salt intrusion length combined with a relatively high extraction rate. Under these conditions an alternated pumping scheme can lead to a larger extraction volume compared to the situation where the pumps are in constant operation and suddenly needs to be turned off. This is the case because the advective transport of salt by the river is much faster than the process of effective dispersion.

The last recommendation is to monitor the additional salt sources, which causes irregularities in salinity distribution. Once these sources are located it is possible to control the flushing of saline water into the river by making use of small structures (e.g. sluices).

1. Introduction

1.1 Estuary description

The Pungue river originates in the Eastern Highlands of Zimbabwe and then flows eastward through Mozambique. The river drains in the Indian Ocean at Beira city creating a large alluvial estuary (see figure 1). The definition of an estuary is nicely given by Dionne (1963): “an inlet of the sea reaching into the river valley as far as the upper limit of tidal rise”. In other words it is the transition where the river meets the sea. The Pungue river has a length of 400 km and it drains a basin of around 31,000 km². Only 5% of the drained area is located in Zimbabwe, nevertheless a considerable part (28 %) of the discharge is generated here (Graas, 2002; SWECO & Associates, 2004; Terink & Droogers, 2014; Zanting, Macueve, & Novela, 1994).

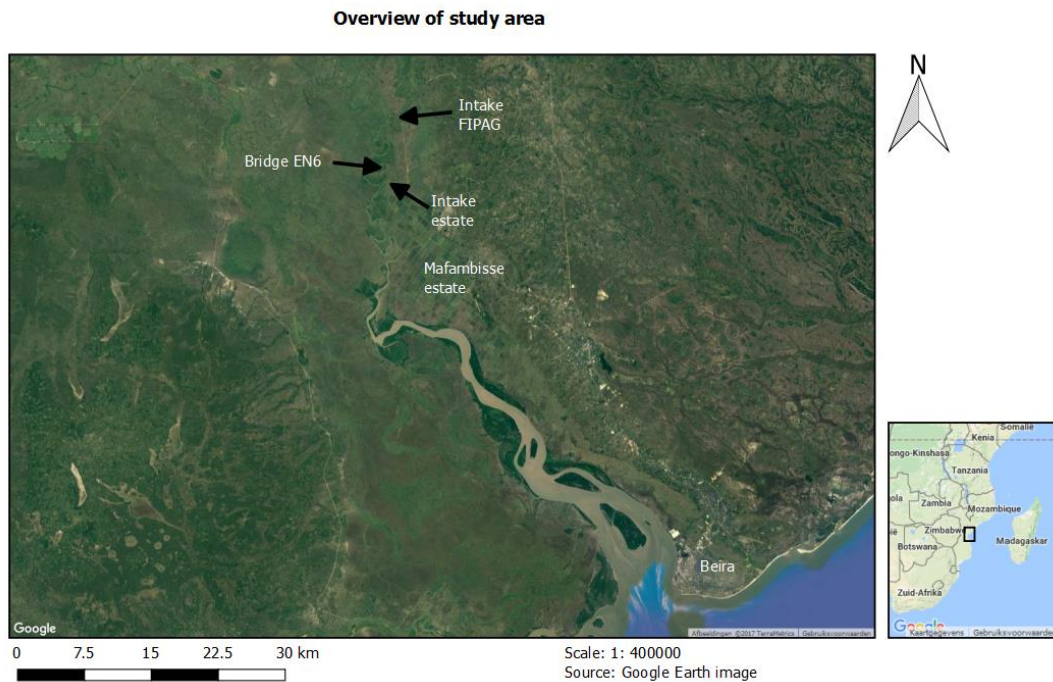


Figure 1: overview of the Pungue estuary and relevant locations

The local population living in the area of the estuary are dependent on the Pungue as source for food by fishing, but also as a source of fresh water for irrigation purposes. Historical data of ARA-Centro shows that the discharge of the river, near the bridge of the EN6, can roughly vary between 10m³/s – 1000 m³/s dependent on wet or dry season.

There are two main commercial fresh water consumers, namely FIPAG (local drinking water company) and the sugarcane estate of Mafambisse. The sugarcane estate is located approximately 50 km from the city of Beira and has a size of approximately 9000 ha. The water intake of the estate is located in the north, roughly 80 km from the mouth of the river. The plantation uses the fresh water from the river for irrigation and process purposes. They extract around 500,000 m³/day from the river Pungue.

The other major consumer is the local drinking water company FIPAG, which provides the city of Beira of drinking water. The FIPAG water intake is located approximately 90 km from the estuary mouth, which is significantly further then the Mafambisse pumping station. Therefore the intake of FIPAG is less sensitive to salt water intrusion. FIPAG extracts around 50,000 m³/day from the river to meet the drinking water needs of Beira.

1.2 Problem statement

The Mafambisse sugarcane estate is dependent on fresh water from the river Pungue for irrigation and process purposes. In the dry season the river discharge can become very low due to droughts in Mozambique and Zimbabwe. In combination with a high tidal range this will result in a large salt intrusion, which can lead to high salinity values at the intake of the estate. If the salinity exceeds the threshold of 0.16 kg/m^3 the water cannot be taken in, without seriously affecting the yield or the operation of the sugar factory.

1.3 Research objective

The main objective of this research is:

Obtain a thorough insight in the characteristics of the salt intrusion in the Pungue estuary in order to give preliminary solutions to the sugarcane estate at Mafambisse, which measures can be taken to minimize the salt incidents at the water intake.

In order to achieve this objective the following aspects need to be taken into account:

- Measure and describe the hydraulic characteristics of the estuary such as: the tide, river discharge, depth profiles and the process of salt intrusion.
- Elaborate on the steady and unsteady state model developed by Savenije for describing the salt intrusion in alluvial estuaries.
- Develop various scenarios with different extraction rates, river discharge and bend cut offs.
- Provide the estate with preliminary solutions for minimizing the salt incidents at the intake.

2. Theory on salt intrusion

This study applies the Rapid Assessment Technique for Salt Intrusion in Alluvial Estuaries developed by Savenije (1992b). The method is based on balance equations of mass, salt and sediment transport processes observed in alluvial estuaries. The following subchapters provide a short summary of the essential assumptions and equations of the book *Salinity and Tides* (Savenije, 2012) and the corresponding papers (Savenije, 1986, 1988, 1989, 1992b, 1993; Savenije & Pagès, 1992a), which elaborate in more detail on the Rapid Assessment Technique for Salt Intrusion in Alluvial Estuaries.

2.1 Geometry alluvial estuaries

In an estuary there are many drivers that affect the characteristics of an estuary. In order to understand these characteristics it is important to understand the dominant processes. These dominant processes are: the tide, river discharge, waves, sediment transport, density difference and the climate (Savenije, 2012).

In alluvial estuaries the bed consists of both riverine and marine sediment and one could state they have movable beds. The shape of an estuary is directly related to its hydraulics. So the water movement in an alluvial estuary depends on the topography and the topography depends, on the other hand on the power of the hydraulics.

The banks of alluvial estuaries are converging and can be described by an exponential function. Moreover, the longitudinal variation of the cross-section therefore can also be described exponentially. The rate of convergence can then be expressed by a length scale called: the convergence length.

$$A(x) = A_0 \exp\left(-\frac{x}{a}\right) \quad (2.1)$$

$$B(x) = B_0 \exp\left(-\frac{x}{b}\right) \quad (2.2)$$

With:

A	= Tidal average cross-sectional area	[m ²]
A_0	= Cross-sectional area at the estuary mouth	[m ²]
a	= Cross-sectional convergence length	[m]
x	= Distance from the estuary mouth	[m]
B	= Tidal average estuary width	[m]
B_0	= Width at the estuary mouth	[m]
b	= Width convergence length	[m]

In this research the cross-sectional area will be described by an exponential function along the estuary axis, where the x-axis point in upstream direction and $x=0$ is positioned at the mouth of the estuary. The depth can be expressed as follows:

$$h(x) = h_0 \exp\left(\frac{x(a-b)}{ab}\right) \quad (2.3)$$

With:

h	= Tidal average depth	[m]
h_0	= Depth at the estuary mouth	[m]

In the special case where the two convergence lengths a and b are equal the above equation simplifies to $h=h_0$. When the convergence of the banks compensates for the dissipation of energy caused by friction the tidal range is constant over the estuary length. The situation where $a = b$ is called an ideal estuary and observations made by the authors shows that this is a reasonable assumption for the Pungue estuary.

2.2 The tidal wave

To understand the character of an estuary it is important to understand one of its main drivers: the tide. Tides are generated by the interactions between the moon, sun and earth. The gravitational forces exerted by the moon and sun combined with the earth's rotation causes the fall and rise of the sea levels. The tide brings a lot of energy and salt in the estuary system and therefore it is of great importance. The harmonic character of the tide is responsible for pumping of water into or out of an estuary. This erosive power can only be compensated by bank convergence where the rate of convergence can be described exponentially (Savenije, 2012).

The tide in the Pungue estuary has a diurnal character. This means that high water and low water occur twice during a day. The corresponding tidal period is equal to 12 hours and 20 minutes; this is the duration of one tidal cycle.

The tide in an alluvial estuary propagates as a wave of mixed character. It contains mixed elements of both a progressive and a standing wave. The phase lag ε between water level and flow velocity varies between 0 and $\pi/2$, this corresponds with a slack time between 0 and 185 minutes after LW or respectively HW. As can be seen from figure 2 high water slack (HWS) occurs after high water (HW) and low water slack (LWS) occurs after low water (LW) and both occur before the mean tidal level. Slack is the moment just before the flow changes direction during that moment there is no current. During HWS the salt intrusion is at its maximum and during LWS minimum.

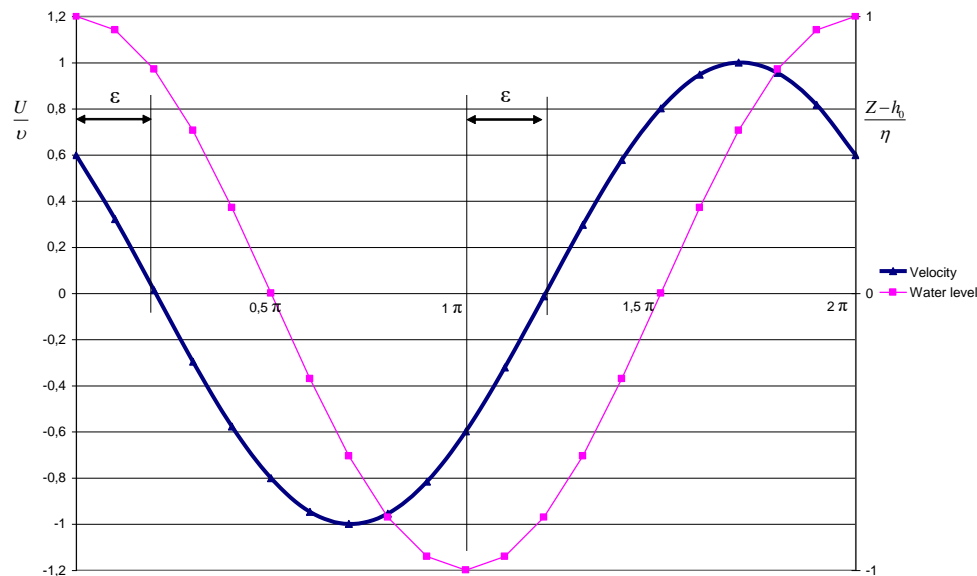


Figure 2: mixed wave showing the phase lag between LW and LWS, and between HW and HWS (Savenije, 2006)

With the tidal wave equations the celerity, slack times, excursion length and dampening factor of the tide in the Pungue estuary can be calculated. These equations are no further explained in this report, for explanation and derivation of these equations the authors refer to the book Salinity and Tides (Savenije, 2012).

2.3 Mixing processes in alluvial estuaries

This subchapter gives a short introduction on the mixing of fresh and salt water processes and its corresponding mechanisms. It also presents a formula for longitudinal dispersion, which is needed for the derivation of the steady and unsteady state salt intrusion model presented in subchapters 2.4 and 2.5.

According to Savenije the following processes drive longitudinal effective dispersion of salinity: the tidal shear, residual currents, density current, mixing by trapping and turbulent mixing. For an elaborate description of these processes and their relevant importance to effective longitudinal dispersion the authors refer to chapter 4 of Salinity and Tides (Savenije, 2012).

Longitudinal effective dispersion of salinity can be described as the process of a moving water particle and its interaction with other particles, averaged over a certain time period. Effective dispersion counteracts the advective salt transport. If an estuary is positive the salinity decreases in upstream direction, and the dispersion mechanisms result in an inward transport of salt. If the advective transport is equally strong as the longitudinal effective dispersion a tidal-averaged equilibrium can be reached. This is important to understand in order to derive an expression for the dispersion coefficient (D).

Salinity and Tides (Savenije, 2012) presents a general formula for longitudinal dispersion, which is based on the Van der Burgh's equation. The formula is corrected for the exponential variation of the cross-section as assumed in section 2.1. The equation is given as follows:

$$\frac{D}{D_0} = 1 - \beta \left(\exp\left(\frac{x}{a}\right) - 1 \right) \quad (2.4)$$

$$\beta = \frac{KaQ_f}{D_0A_0} \quad (2.5)$$

With:

D = Tidal average longitudinal dispersion	[m ² /s]
D_0 = Dispersion coefficient at the estuary mouth	[m ² /s]
x = Distance from the estuary mouth	[m]
a = Cross-sectional convergence length	[m]
β = Dispersion reduction rate	[-]
K = Van der Burgh's coefficient	[-]
Q_f = Fresh river discharge	[m ³ /s]
A_0 = Cross-sectional area at the estuary mouth	[m ²]

This is a simple equation, which links the longitudinal effective dispersion to the geometry of the estuary and the river discharge. The geometry is clearly present via the convergence length a and the cross-sectional area at the mouth of the estuary A_0 . In order to use these formulas in a predictive way it is necessary to find an estimate for D_0 and K , in which the latter represents the Van der Burgh's constant.

The Van der Burgh's coefficient can be seen as a "shape factor", which is influencing the shape of the salt intrusion curve. Alluvial estuaries and in particular the Pungue estuary can be seen as a well-mixed estuary, because the tidal flow is relatively large compared to the fresh water discharge. This assumption that the Pungue estuary is well mixed is strengthened by the fact that during the dry season the water demand is at its highest and the availability at the lowest possible point. In the dry season the estuary behaves definitely as a well-mixed estuary and this is in most cases the period of interest, because water managers are often interested in the extremes.

Well-mixed estuaries can have different shapes of salt intrusion curves. This strongly depends on the topography of an estuary. The Pungue estuary has a salt intrusion curve in the shape of a dome, which is mainly due to its funnel shaped topography. If one would plot the salinity S in $[\text{kg}/\text{m}^3]$ against x in $[\text{km}]$, where x is the distance from the estuary mouth the dome shaped intrusion curve becomes clearly visible:

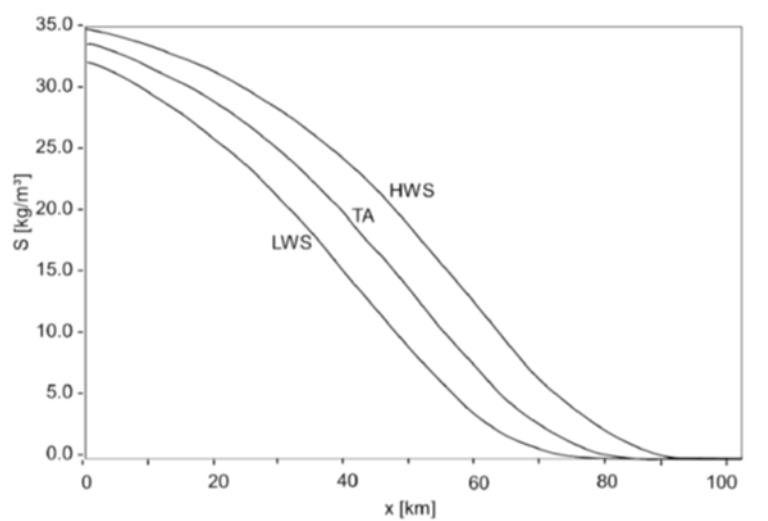


Figure 3: definition salt intrusion curve and plotted LWS, TA and HWS situation

In the figure above three different salt intrusion curves are plotted. Where LWS stands for low water slack and corresponds with the salt intrusion during the moment of low water slack. HWS stands for the salt intrusion during the moment of high water slack. In between low water and high water slack the tidal average situation is plotted, which shows the salt intrusion averaged over one tidal cycle.

To elaborate further on the formula presented for longitudinal dispersion, predictive formulas need to be found for D_0 and respectively K . Savenije did a lot of observations in a large number of estuaries worldwide and came up with the following expressions for D_0 and K :

$$D_0 = 1400 \frac{h_0}{a} \left(\frac{\Delta\rho}{\rho} g h_0 \frac{Q_0 T}{P} \right)^{0.5} E_0 \quad (2.6)$$

$$K = 0.3 * 10^{-3} \left(\frac{E}{H} \right)^{0.65} \left(\frac{E}{C^2} \right)^{0.39} (1 - \delta b)^{-2.0} \left(\frac{b}{a} \right)^{0.58} \left(\frac{E a}{A_0} \right)^{0.14} \quad (2.7)$$

With:

D_0 = Dispersion coefficient at the estuary mouth	[m ² /s]
h_0 = Depth at the estuary mouth	[m]
a = Cross-sectional convergence length	[m]
$\Delta\rho$ = Density difference between salt and fresh water	[kg/m ³]
ρ = Density of fresh water	[kg/m ³]
g = Gravitational acceleration	[m/s ²]
Q_0 = Fresh water discharge during dry season	[m ³ /s]
T = Tidal period	[s]
P = Wetted perimeter	[m]
E_0 = Tidal excursion at the estuary mouth	[m]
K = Van der Burgh's coefficient	[-]
E = Tidal excursion	[m]
H = Tidal range	[m]
C = Chézy coefficient	[m ^{0.5} /s]
δ = Damping number	[-]
b = Width convergence length	[m]
A_0 = Cross-sectional area at the estuary mouth	[m ²]

It should be mentioned that the predictive formula for the Van der Burgh's coefficient K should be used carefully. In reality the value should always be between zero and unity, which does not become clear immediately from the formula. The predictive value of K is weak and therefore it is important to use it as a first estimate. In this research a value of K is obtained empirically by applying a moving-boat survey on a HWS and LWS situation. The moving-boat survey will be explained in more detail in chapter 3: description of the study.

2.4 Steady state model

An estuary can be seen as the transition between a river and a sea. Where the sea is responsible for the supply of salt water into the estuary and the (fresh) river discharge tries to push the salt back into the ocean. If these two processes are in balance the estuary is in steady state, which results in a steady decreasing salt intrusion curve. It starts with a value being roughly the same as sea salinity and gradually approaches to river salinity, after salt intrusion length has been reached (as can be seen in figure 3).

The most important assumption of a steady state model assumes that the time dependent component d/dt in the salt balance equation becomes zero. This is reasonable if you average the salt concentrations over a period of time. The boundary conditions such as river discharge and tidal range will become constant.

The steady state salt balance which is described in the book *Salinity and Tides* (Savenije, 2012) is based on the salt balance equation. It can be elaborated to a 1-D steady state salt balance, which is given as follows:

$$S_i - S_f = -\frac{A}{Q_f} D_i \frac{dS_i}{dx} \quad (2.8)$$

Where subscript i indicates the HWS, TA or LWS condition. Depending on the situation of interest. In this research the HWS situation is the most interesting situation while the salt intrusion is then at its maximum.

With:

S_i = Salinity during HWS, TA or LWS condition	[kg/m ³]
S_f = Fresh water salinity	[kg/m ³]
A = Tidal average cross-sectional area	[m ²]
Q_f = Fresh water discharge	[m ³ /s]
D_i = Dispersion coefficient during HWS, TA or LWS	[m ² /s]
x = Distance from the estuary mouth	[m]

This formula can be rewritten to an analytical solution of the steady state model:

$$S(x) = (S_0 - S_f) \left(\frac{D(x)}{D_0} \right)^{\frac{1}{K}} + S_f \quad (2.9)$$

With:

$S(x)$ = Salinity as a function of x	[kg/m ³]
S_0 = Sea salinity	[kg/m ³]
S_f = Fresh water salinity	[kg/m ³]
$D(x)$ = Dispersion coefficient as a function of x	[m ² /s]
D_0 = Dispersion coefficient at the estuary mouth	[m ² /s]
K = Van der Burgh's coefficient	[-]

This formula is used to calculate the salinity distribution along the x –axis of the estuary averaged over the tidal period. In other words it is the mean salt concentration over one tidal cycle. The maximum salt concentrations occur at HWS and the minimum salt concentrations at LWS. To get the TA situation the salt intrusion curve is shifted with approximately half of the excursion length.

The salt intrusion curves depend on four calibration parameters: Van der Burgh's coefficient (K), dispersion coefficient at the mouth (D_0), (fresh) river discharge (Q_f) and the tidal excursion length at the estuary mouth (E_0). These parameters are obtained by calibrating the steady state model with measurements in the field (moving-boat method).

2.5 Unsteady state model

This paragraph begins with explaining briefly the theory and equations of the unsteady state model. Afterwards two applications of the unsteady state model will be introduced.

2.5.1 Theory of unsteady state model

The steady state model only holds when the changes in discharge are not too big over time. When the discharge changes due to natural (storm events or droughts) or human interactions this will result in a shift in the salt intrusion curve upstream or downstream. After some time the estuary will reach a new steady state. It differs from estuary to estuary how long it takes to adapt due to changes in discharge. Some estuaries will never reach a steady state due to regular changes in discharge or very long adaptation timescales. To get more insight in the salt intrusion curves between two steady states and the time it takes to reach a new steady state an unsteady state salt intrusion model will be used. Of course the big difference of this model is that the assumption d/dt is equal to zero cannot be used anymore. This means that the salinity is dependent on the location from the mouth (x) and on the time (t).

In order to develop an unsteady state model one should take a look into the one-dimensional unsteady state salt balance equation:

$$r_s A \frac{\partial s}{\partial t} + (Q_t - Q_f) \frac{\partial s}{\partial x} - \frac{\partial}{\partial x} \left(AD \frac{\partial s}{\partial x} \right) = -sR_s \quad (2.10)$$

With:

r_s = Storage width ratio	[-]
A = Tidal average cross-sectional area	[m ²]
$s = s(x, t)$ is the salinity	[kg/m ³]
t = Time	[s]
Q_t = Tidal discharge	[m ³ /s]
Q_f = Fresh water discharge	[m ³ /s]
x = Distance from the estuary mouth	[m]
$D = D(x, t)$ is the longitudinal dispersion coefficient	[m ² /s]
R_s = Source term	[m ² /s]

Also the expression of Van der Burgh's equation justified for HWS, LWS and TA conditions is needed to derive an expression for an unsteady state salt intrusion model. Van der Burgh's expression for HWS, LWS and TA conditions is given as follows:

$$\frac{dD_i}{dx} = -K \frac{Q_f}{A} \quad (2.11)$$

With:

D_i = Dispersion coefficient during HWS, TA or LWS	[m ² /s]
x = Distance from the estuary mouth	[m]
K = Van der Burgh's coefficient	[-]
Q_f = Fresh water discharge	[m ³ /s]
A = Tidal average cross-sectional area	[m ²]

The one-dimensional unsteady state salt balance equation can be combined with the Van der Burgh's equation justified for HWS, LWS and TA conditions. These formulas combined lead to the following simplified expression:

$$r_s \frac{\partial s}{\partial t} - q \frac{\partial s}{\partial x} - D \frac{\partial^2 s}{\partial x^2} + r_s \frac{P_n}{h_0} s = 0 \quad (2.12)$$

Where q is equal to:

$$q = (1 - K) \frac{Q_r + r_s B P_n b}{A} - \frac{D}{a} \quad (2.13)$$

With:

r_s = Storage width ratio	[-]
$s = s(x, t)$ is the salinity	[kg/m ³]
t = Time	[s]
q = Coefficient of the advective term	[m/s]
x = Distance from the estuary mouth	[m]
$D = D(x, t)$ is the longitudinal dispersion coefficient	[m ² /s]
P_n = Net rainfall in an estuary	[m/s]
h_0 = Depth at the estuary mouth	[m]
K = Van der Burgh's coefficient	[-]
Q_r = The river discharge	[m ³ /s]
B = Tidal average estuary width	[m]
b = Width convergence length	[m]
A = Tidal average cross-sectional area	[m ²]
a = Cross-sectional convergence length	[m]

The steady state model and the unsteady state model are both based on the one-dimensional salt balance equation. In this equation the first term determines the temporal variability. This term is neglected in the steady state model, but in the unsteady state model this term plays an important role. This will make it no longer possible to solve the one-dimensional salt balance equation analytically, so a numerical scheme has to be used.

The unsteady state model is solved by a Fortran code which is written by Savenije (1988). In this code a six point implicit finite difference scheme which is suggested by Fischer (1972) is used to solve the salt balance equations.

For more information about the unsteady state model and its applicability the authors refer to Savenije (1986), Savenije (1988) and Savenije (1992b).

2.5.2 Application of unsteady state model

In chapter 4.3.3 the unsteady state model will be applied to simulate the effect of an additional salt source. This is only possible in the unsteady state model because the salt source is only active over a certain time period. And the unsteady state model is a numerical model which makes it possible to add the salt source only over a certain range of cells, in this case from $x = 50$ kilometres to $x = 64$ kilometres.

In chapter 4.3.4 the unsteady state model will be applied to simulate the effect of alternated pumping. The theory which support alternated pumping is described in the book *Salinity and Tides* (Savenije, 2012). The theory is that an estuary reacts quicker to an increase in discharge than to a decrease in discharge. This means that if you increase the upstream river discharge by shutting off the pumps at the intake this will lead to an added volume of fresh water, which flushes the salt more downstream (advective process). If the pumps are turned on again the salinization of the estuary (dispersion process) happens at a significantly slower speed. Previous research of Hegnauer and Savenije (2009) in the Pungue estuary shows that alternated pumping can reduce the salt intrusion length. Hegnauer and Savenije (2009) show in their research with virtual experiments that almost twice the amount of water can be extracted with alternated pumping in comparison with a constant extraction rate. Sanders and Piasecki (2002) also show that with an alternated pumping strategy more freshwater can be extracted from an estuary.

3. Description of the study

In order to use the steady and unsteady state model, presented in the previous chapter, values are needed for the model parameters. This chapter provides a description of the data collected during the field study carried out by the authors in November and December of 2016. The following activities will be described: determination estuary geometry, measuring river discharge and the salinity measurements.

3.1 Estuary geometry

To determine the geometry parameters as discussed in chapter 2 a cross-sectional survey has been carried out on the 21st of December. To carry out the cross-sectional survey a motorised boat has been used in combination with a Garmin depth sounder/fish finder/GPS of the type Striker. The depth sounder transmits an acoustic signal and is reflected by the bottom, or any other disturbance under the sounder, and afterwards the signal is collected by the receiver. The time the signal takes between sending and receiving of the acoustic wave is then translated into a depth. The measurements over the cross-section are done from bank to bank and the distance is divided into intervals being roughly of the same length. Due to the large width of the estuary at the mouth the intervals taken here are bigger compared to the other cross-sections.

3.2 River discharge

To calibrate the steady and unsteady state model the river discharge is needed. In this research a discharge measurement has been carried out at the bridge of the EN6 over the Pungue on the 14th of December. The bridge is situated approximately 100 km from the mouth, this location is chosen because the tidal influence is low. So it can be assumed that the measured discharge is roughly equal to the river discharge. The discharge measurement is conducted with an Acoustic Doppler Current Meter (ADCP) also called the River Surveyor.

3.3 Salinity measurements

In order to calibrate and verify both salinity intrusion models, measurements of salinity throughout the estuary have been conducted. In this research two methods are used to collect salinity measurements: the moving-boat method has been applied and use is made of CTD divers.

A CTD-diver is a small measuring device installed under water. It measures: the water temperature, pressure and electrical conductivity over time. It continuously logs this information on a memory unit inside the device. It is possible to set a measuring interval; this can for example be seconds, minutes or hours.

In this research six divers have been installed at strategic locations in the estuary (see figure 4). Because it measures the electrical conductivity it can be used to plot salinity intrusion curves. Another advantage of a CTD-diver is that it logs the water pressure. HW and LW then become clearly visible. If one would install divers at different distances from the mouth the water levels calculated from the pressures can show how much the estuary is dampened. This is a very important parameter needed to solve the tidal wave equations and to come up with an estimate for the phase lack, slack time, celerity and tidal excursion.

The moving-boat method is a method to measure the salt intrusion curve in an estuary. The method means that a boat travels along the estuary with HWS or LWS with the same celerity as the tidal wave. During this transect the salt concentration is measured over several verticals with intervals of 5 to 10 kilometres. This measurement is done with an electrical conductivity meter at HWS or LWS when the current is zero and the salt concentration is locally at its maximum or respectively minimum during LWS. Important for this method is the availability of a boat, which has a speed superior to the celerity of the tidal wave. The moving-boat method is conducted on the 15th, 16th and 17th of December 2016, which was a period around spring tide. During spring tide the tidal range and the salt intrusion are maximum. On the 15th of December a LWS measurement was conducted. Due to some issues with the boat it was not feasible to do a HWS measurement on the 15th of December. On the 16th and 17th of December HWS measurements have been carried out. Due to the limited sun hours and a high chance to get stuck during LWS only the HWS curves are verified on the 16th and 17th of December.

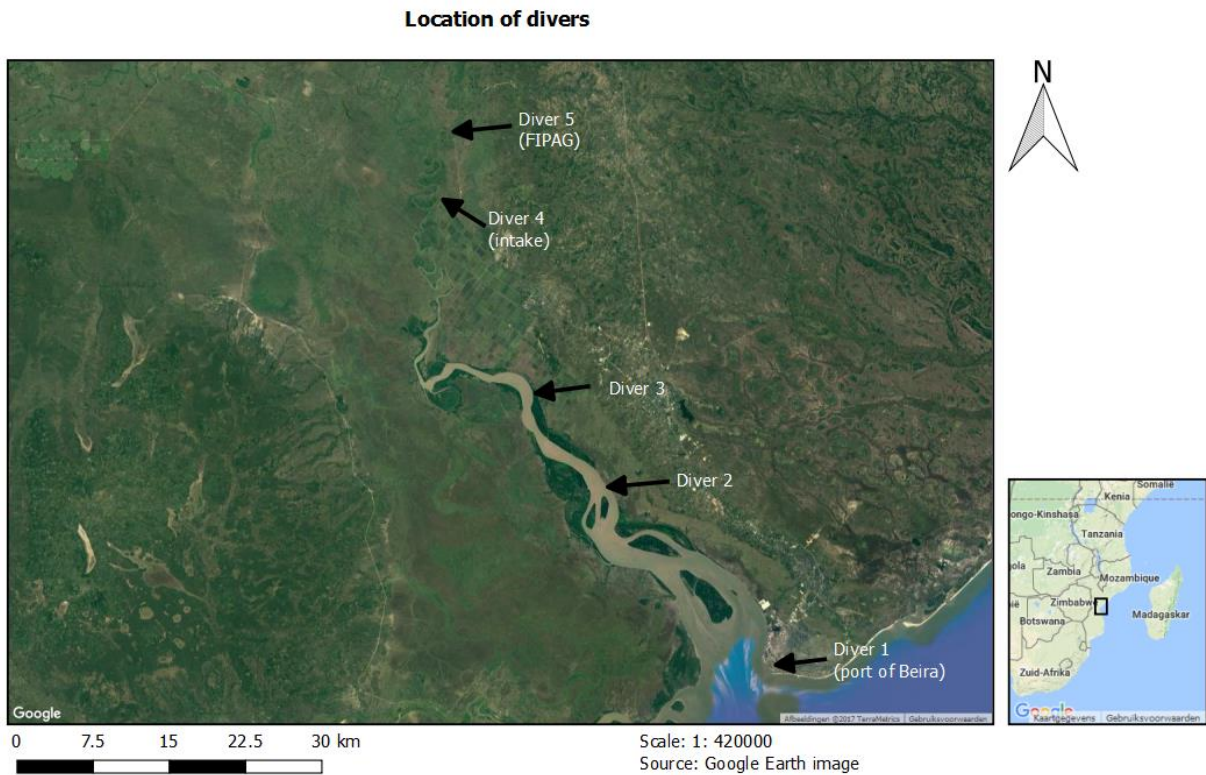


Figure 4: locations of the installed divers

4. Elaboration on salt intrusion models

In this chapter the results are shown from the geometry, salinity and discharge measurements conducted during fieldwork in December 2016. First of all the determination of the geometry parameters will be discussed followed by the application and calibration of the steady state salt intrusion model. After the calibration irregularities measured in the salt distribution will be explained. After calibration of the unsteady state model these irregularities will be modelled with an additional salt source. An example calculation of the additional salinity source is added. This chapter will be concluded with a virtual experiment of alternated pumping.

4.1 Determination estuary geometry

First of all the geometry of the Pungue estuary will be determined. As explained in the previous chapter depth measurements over the cross-section are conducted with a Garmin echo sounder. To correct these depth measurements for a tidal average situation they are corrected with the height of the tidal wave (η) at that specific moment in time. The height of the tidal wave (η) is estimated by data from tide tables, which predict the tidal ranges in Beira hourly (Flater, 1998). This information in combination with measurements conducted by the divers is used to estimate the dampening in the estuary and celerity of the tidal wave. Once this is known the height of the tidal wave can be estimated as a function of the distance x from the mouth and the time t . See appendix A for the measured depths (corrected by η), widths and cross-sections.

In order to obtain the width and cross-sectional convergence lengths, the corrected depth measurements and width measurements (obtained with Google Earth in intervals of 2,5 km) are plotted in figure 5. The measurements of the depth and width as well as the calculated cross-sectional areas are plotted on semi-logarithmic paper. To find out if it is necessary to model the Pungue estuary in one or multiple branches the width measurements are corrected by subtracting the river width (B_r). This means that the calculated cross-sectional areas (A) also have to be corrected by subtracting the cross-sectional area of the river (A_r). Figure 5 shows the corrected values for the widths, depths and cross-sectional areas (see also appendix A). As can be seen from figure 5 there are no significant inflection points visible, which means that the Pungue estuary can be well represented by one branch. To get values for the width and cross-sectional convergence lengths an exponential trend line is added through the different data points. The slopes of these trend lines represent respectively the width and cross-sectional convergence lengths. The obtained geometry parameters are summarised below.

Table 1: geometry parameters

Geometry parameters	a [m]	b [m]	B_0 [m]	A_0 [m ²]	h_0 [m]	\bar{h} [m]
Pungue	12255	13680	7154	36271	5.1	3.4

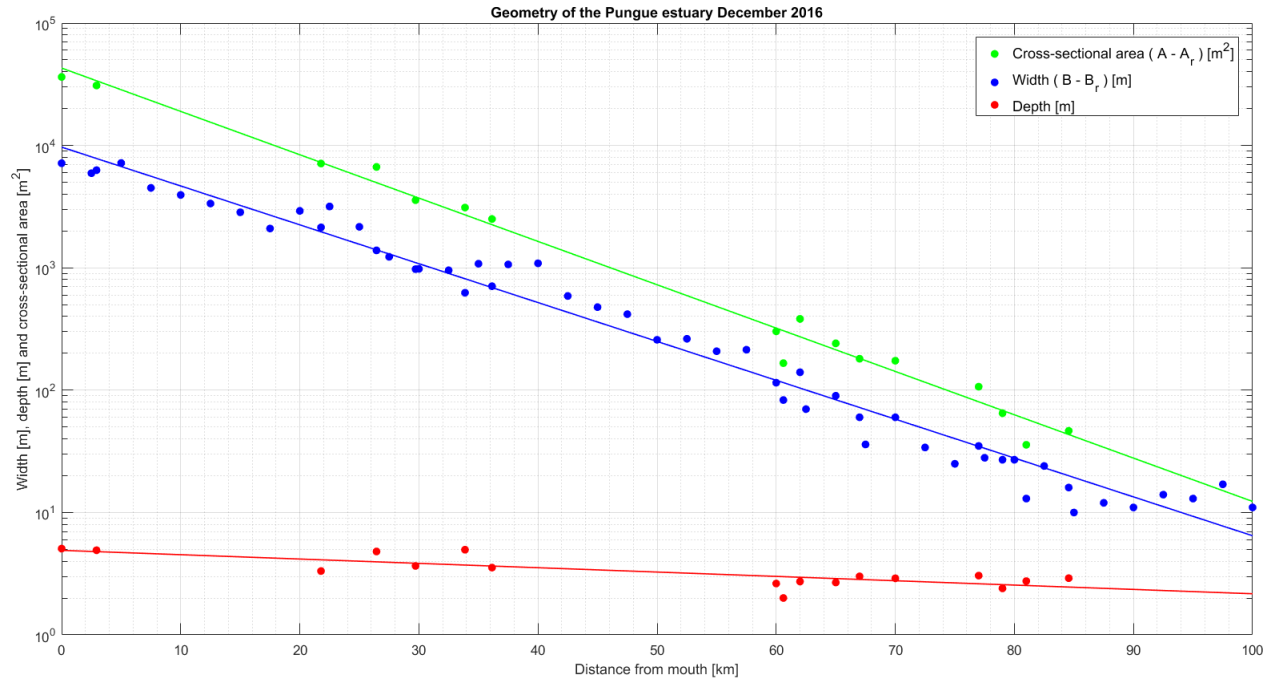


Figure 5: corrected widths, depths and cross-sectional areas for tidal average situation

4.2 Application steady state model

To be able to predict different salt intrusion curves for different scenarios (chapter 5), the possibilities to use a steady state model needs to be explored. This will be done in this subchapter. The steady state model as presented in chapter 2 will be calibrated on the salinity measurements conducted with the moving-boat method on the 15th, 16th and 17th of December 2016. After the calibration of the steady state model this chapter discusses the possible applications of the unsteady state model and its corresponding advantage to add an additional source of salt.

4.2.1 Calibration steady state model

On the website of Salinity and Tides the steady state model developed by Savenije is available as open source software. Applications of the model can be found on multiple estuaries all over the world. In order to understand this chapter it is recommended, by the authors of this research, that the readers of this document open the open access spread sheets of the Pungue on <https://salinityandtides.com/applications/>.

The steady state model can be calibrated by the following calibration parameters: Van den Burgh's coefficient (K), the dispersion at the estuary mouth (D_0), the river discharge (Q_f) and the convergence excursion (e) of which the latter is an expression of the extent of the dampening of the tidal excursion.

The model is calibrated on the salinity measurements conducted with the divers and the moving-boat method. The result is shown below:

Table 2: values of the calibration parameters for the steady state model

Calibration parameters	K [-]	D_0 [m ² /s]	Q_f [m ³ /s]	e [m]
Pungue	0.2	450	28	150000

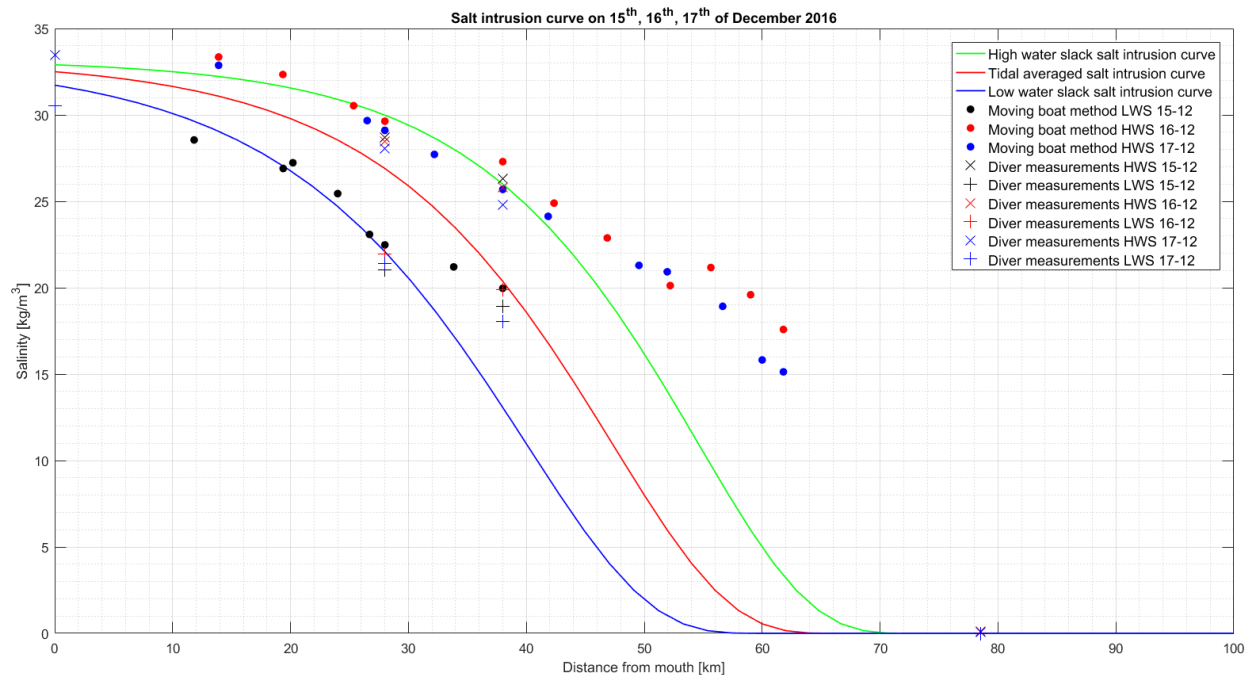


Figure 6: steady state simulation and moving-boat measurements on the 15th, 16th and 17th of December 2016

In figure 6 the steady state salt intrusion curves for LWS, TA and HWS conditions are plotted. The graph shows that the maximum salt intrusion length during the measurement period is around 71 kilometres from the mouth. During these days the river discharge was 32 m³/s (measured by an ADCP). The estate was extracting on average 4 m³/s, which results in a river discharge of 28 m³/s downstream of the intake. This discharge is used as input for the steady state model.

Based on the measurements the values of D_0 and K are calibrated on respectively 450 m²/s and 0.2. This value of 0.2 for the Van der Burgh's coefficient is used as an estuary characteristic and is therefore used in chapter 5 for the development of different scenarios.

In figure 6 it is clearly visible that from $x = 40$ km up to $x = 60$ km the measurements of HWS show a different behaviour in salinity distribution compared to the line of the steady state model representing the HWS situation. The salinity values measured by the moving-boat method are here significantly higher. In the following subchapter possible causes for these irregularities in salinity distribution will be introduced.

4.2.2 Irregularities in salinity measurements

In this subchapter possible explanations will be given for the sudden increase in salinity between $x = 40$ km and $x = 60$ km, which can be observed in figure 6. When analysing the increase in salinity one could think of different reasons resulting in higher salinity values. For example when evaporation would exceed rainfall and runoff, it is possible hypersalinity occurs in an estuary. In this case the dispersive transport of salt is dominant over the advective transport. In other words the supply of fresh water in this situation is too low to flush the salt accumulation caused by evaporation. Hypersalinity is a known phenomenon in shallow estuaries (Savenije & Pagès, 1992a). However the Pungue estuary is not shallow and most of the time (even during dry season) there is enough fresh water available to flush the estuary. Hypersalinity can therefore be discarded as an explanation for the observed increase in salinity values.

As can be seen from figure 6 the salinity values drop rapidly after $x = 60$ km and decrease to river salinity. This suggests that there is a local source of salt, which is adding highly saline water to the river and is spread out over time. This would explain why the salinity values over the river section $x = 40$ km and $x = 60$ km are higher than expected but decrease to river salinity after this section. It is likely that this phenomenon occurs in the Pungue estuary and therefore two explanations will be given where this additional source of salt can originate from:

- 1) **Flushing of saline (unused) areas:** As shown in figure 7 some plots next to the left bank (East) are not in use. These grounds were used to cultivate sugarcane, but are abandoned at the moment. Mainly due to the bad soil conditions caused by salinization and soil depletion. These abandoned areas are still connected to the Mafambisse main drainage canal, which is directly in contact with the river. This means that if a serious rain event has happened these bad soils are flushed and the accumulated salt ends up in the river.
- 2) **Flood event:** Another explanation would be a flooding event after a storm surge on the right bank (West), which is not protected by dikes. Once a storm surge occurs it is possible that saline water floods the natural levee and saline water from the Indian Ocean is stored on the land. Subsequently the saline water on the land becomes more saline over time due to evaporation. If there is a severe rain event this water, which is highly saline, can flow back into the river. This could explain the local increase in salinity values. There are some signs that a flood has happened at this location. Figure 8 shows historical images of this floodplain; here it is visible that there has been a shift in land from farmland to bare land, with a white colour.

On the days preceding the boat measurements (15-17th December) indeed intensive rainfall took place, which may have caused the flushing out of the saline water from the bare land.

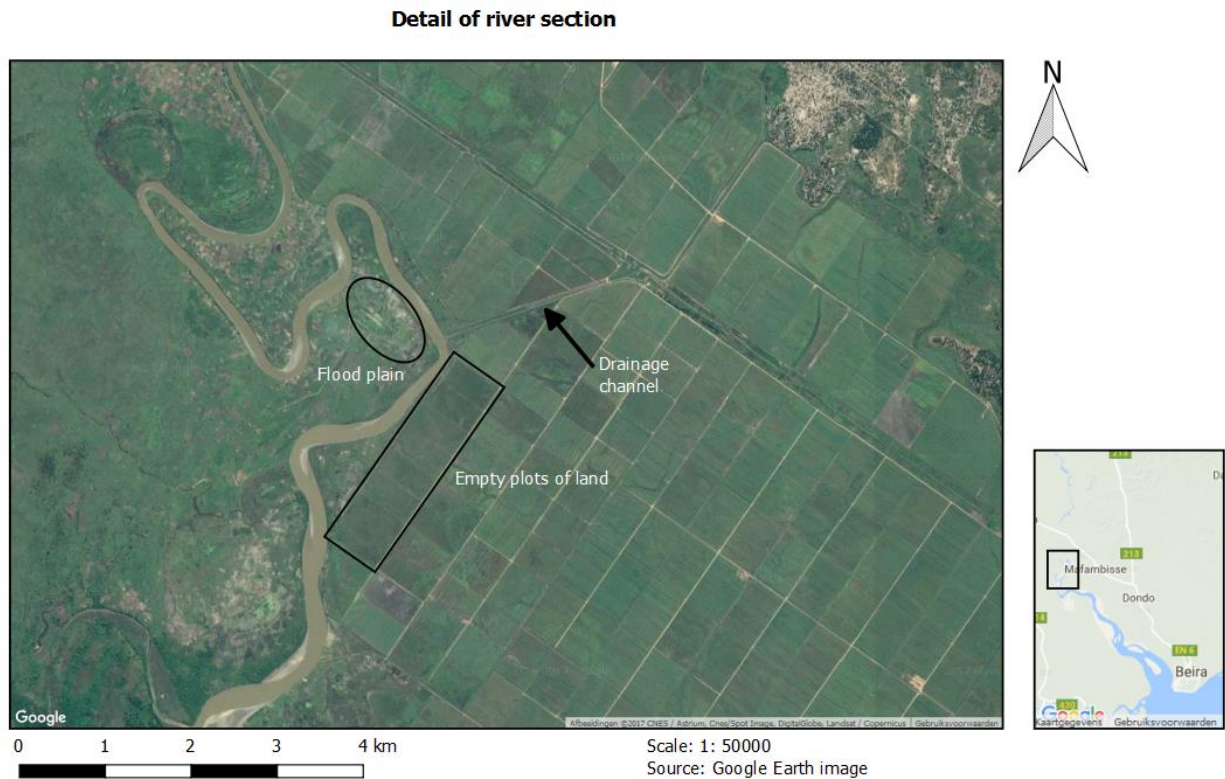


Figure 7: detail of river section with irregular salt distribution between $x = 40$ km to $x = 60$ km from the estuary mouth

To prove that an additional source of salt could be causing the higher observed salinity values use has been made of the unsteady state model. First of all because the steady state model incorporates the time dependency d/dt and the salt is added over a certain period of time. Secondly because the unsteady state model is a numerical model, which makes it possible to add an additional salt source at certain computational cells (over a certain length of the x -axis). How this additional source of salt can be incorporated into the unsteady state model is explained in the following subchapter.

Historical images of river section



Scale: 1: 1000, Source: Google Earth images, Date: 12 - 5 - 2009



Scale: 1: 1000, Source: Google Earth images, Date: 13 - 1 - 2013



Scale: 1: 1000, Source: Google Earth images, Date: 30 - 4 - 2016

Figure 8: historical images of river section where salt is added $x = 40$ km to $x = 60$ km from the estuary mouth.

The first satellite image in figure 8 shows that in 2009 the right bank (West) shows a lot of green, which suggest agricultural activities. Over time this changes and white spots appear. These white spots suggest a change in vegetation as can be clearly noticed from the second and third satellite image.

4.3 Application unsteady state model

Besides the steady state model this research makes use of the unsteady state model as presented in chapter 2. The advantages of the unsteady state model are that it can show the effect of different pumping schemes and that it is possible to add an additional salt source. First the calibration of the unsteady state model will be discussed. Secondly the additional salt source is added to the unsteady state model. After that an example calculation is added to get an indication of how much salt is added locally to the river in order to get the observed irregularities in salt distribution. Finally the unsteady state model will be used to simulate the effect of alternated pumping.

4.3.1 Calibration unsteady state model

The unsteady state model as explained in chapter 2 is used to incorporate the effect of an additional source of salt. The unsteady state model estimates the value for the dispersion coefficient D_0 . And a Van der Burgh's constant K of 0.2 is used. The formula presented in chapter 2.3 is slightly adjusted (calibrated) to the values D_0 obtained by the calibration of the steady state model. A calibration factor of 0.85 is added to the formula developed by Savenije (2012):

$$D_0 = 1400 \frac{h_0}{a} \left(\frac{\Delta\rho}{\rho} g h_0 \frac{Q_0 T}{P} \right)^{0.5} E_0 \mathbf{0.85} \quad (4.1)$$

With:

D_0 = Dispersion coefficient at the estuary mouth	[m ² /s]
h_0 = Depth at the estuary mouth	[m]
a = Cross-sectional convergence length	[m]
$\Delta\rho$ = Density difference between salt and fresh water	[kg/m ³]
ρ = Density of fresh water	[kg/m ³]
g = Gravitational acceleration	[m/s ²]
Q_0 = Fresh water discharge	[m ³ /s]
T = Tidal period	[s]
P = Tidal prism	[m ³]
E_0 = Tidal excursion at the estuary mouth	[m]

4.3.2 Additional salt source in unsteady state model

To incorporate the effect of pumping (by Mafambisse and FIPAG) and to explore the effect of an additional salt source a simulation has been done with the unsteady state model. The outcome of this simulation is shown below:

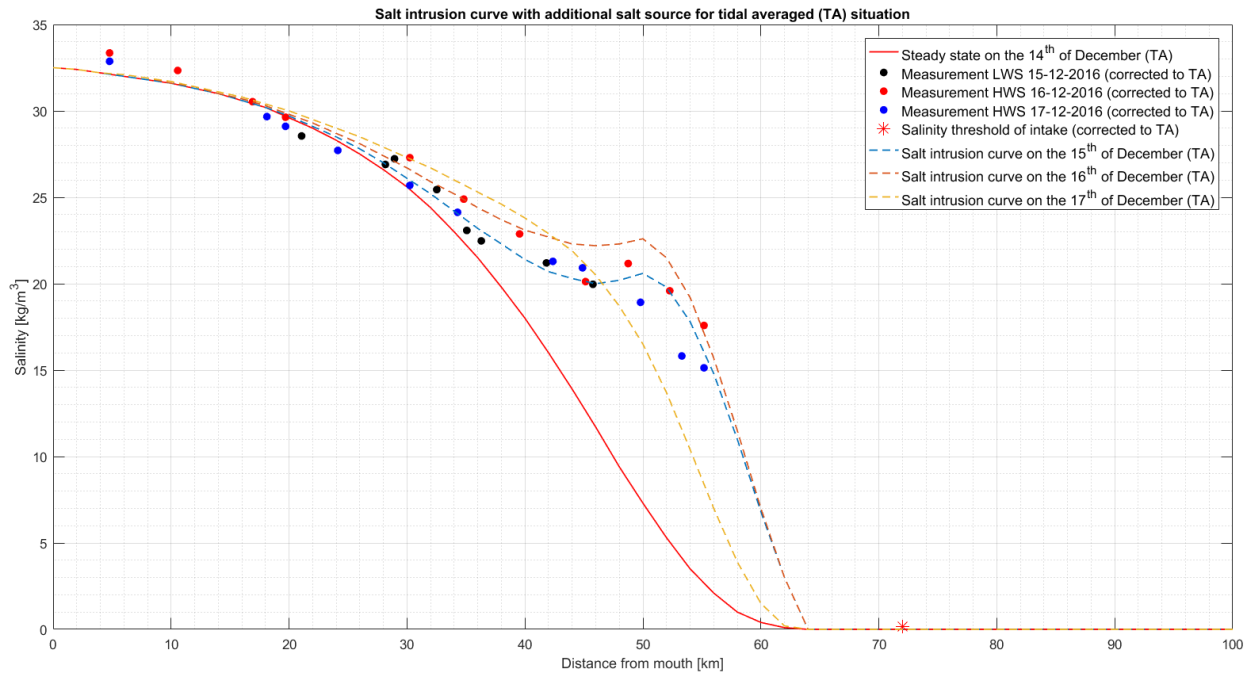


Figure 9: unsteady state simulation with additional salt source for TA situation

The figure shows a simulation where an amount of $11.6 \text{ kg/m}^3/\text{day}$ salt has been added over a distance equal to the tidal excursion (14 km). Note that this is a simulation of the tidal averaged situation; all measurements and the salinity thresholds are corrected to the tidal averaged situation. The additional salt load is applied for 3.5 days (13th, 14th, 15th and part of 16th of December) over the section $x = 50 \text{ km}$ to $x = 64 \text{ km}$. As can be seen from figure 9 the unsteady state model represents the measured salinity values much better compared to the steady state model. So if one would add this constant amount of salt over a period of 3.5 days at this specific river section the model represents quite accurate the measured salinity values. This makes it very likely that additional salt has been flushed into the river during the measurement campaign of the 15th, 16th and 17th of December 2016. The model also shows that after these 3.5 days, when there is no additional salt source, the salt concentrations quickly return to the steady state salt intrusion curve and does not propagate far enough upstream to reach the intake. This shows that this additional salt source only has an effect on the salt concentration during a period of some days after a rain event.

4.3.3 Calculation additional salinity source

First a quick estimate will be made how much salt has to be added by the additional source to get the situation shown in figure 9. This calculation is based on the salt load, which is added in the unsteady state model. Secondly an estimate will be made of the minimum required area and discharge which is needed to deliver this amount of salt. Finally the required net runoff-generation of the two possible salt sources are calculated.

Calculation amount of salt added:

In the unsteady state model a load of $11.6 \text{ kg/m}^3/\text{day}$ is added during 3.5 days:

$$\rightarrow 11.6 \frac{\text{kg}}{\text{m}^3} \cdot 3.5 \text{ days} = 40.6 \frac{\text{kg}}{\text{m}^3} \text{ salt added in total.}$$

This load is added over a length equal to the tidal excursion (14000 m) and the model uses calculation steps of 2000 m, so the salt load is added at 7 cells. The average cross-sectional area at this reach is 250 m^2 (measurement by the ADCP). This leads to:

$$\rightarrow 40.6 \frac{\text{kg}}{\text{m}^3} \cdot \frac{14000}{2000} \cdot 250 \approx 71 \cdot 10^3 \text{ kg of salt added.}$$

Estimate of discharge and area needed for this salt source

The following calculations are based on two assumptions:

1. The concentration of the additional saline water (which originates from the additional salt source) is equal to approximately 20 kg/m^3 . This guess is based on the salt concentrations, which are measured between 50 and 60 kilometres from the mouth (see figure 9).
2. At the area where the additional salt originates from, a layer of water is present of 0.01 m.

With these assumptions an estimate of the area of the additional salt source (A_{salt}) and the discharge from this area (Q) is made:

$$\rightarrow A_{salt} = \frac{71 \cdot 10^3 \text{ kg}}{20 \frac{\text{kg}}{\text{m}^3} \cdot 0.01 \text{ m}} \approx 36 \cdot 10^4 \text{ m}^2$$

$$\rightarrow Q = \frac{71 \cdot 10^3 \text{ kg}}{20 \frac{\text{kg}}{\text{m}^3} \cdot 86400 \text{ seconds} \cdot 3.5 \text{ day}} \approx 0.12 \frac{\text{L}}{\text{s}} \approx 1000 \frac{\text{m}^3}{\text{day}}$$

The areas that are mentioned as a possible source are measured with satellite images (GoogleEarth, 2016). By dividing the discharge (Q) over the area (A) of these sources the net runoff-generation is calculated for each area. The results are:

1. **Flushing of saline (unused) areas:** the unused plots next to the river have a size of roughly 144 hectares. This means that a net runoff-generation of 0.7 mm/day would have been enough to generate a discharge of $1000 \text{ m}^3/\text{day}$.
2. **Flood event:** the flood plain next to the river has a size of approximately $290 \cdot 10^3 \text{ m}^2$. This means that a net runoff-generation of 3.5 mm/day would have been enough to generate a discharge of $1000 \text{ m}^3/\text{day}$.

So based on this estimate both areas are big enough to be the additional salt source. The required net runoff generation at both areas are reasonable.

4.3.4 Virtual experiment alternated pumping

The effects of alternated pumping are best visible when an extreme scenario is taken. Another reason is that alternated pumping will only be necessary if continuously pumping causes a salt intrusion length, which is too large. To test the concept of alternated pumping a scenario is chosen with a river discharge of 20 m³/s downstream of the intake when the pumps are off and 5 m³/s if the pumps are turned on. So in this scenario the extraction rate is 15 m³/s. The pumps are switched on and off with an interval of six hours. This situation is compared with a constant extraction rate of 7.5 m³/s (river discharge of 12.5 m³/s), which results in the same total volume extracted from the Pungue.

The result of this simulation of the unsteady state model is plotted in figure 10. This figure shows that the toe of the salt intrusion curve (between x = 60 km and x = 70 km) reacts quickly to changes in discharge. The rest of the salt intrusion curve (between x = 20 km and x = 60 km) reacts slower. This part of the estuary slowly becomes more saline but the salt concentrations stay below the salt concentrations of the steady state corresponding to the constant extraction rate (green line). Table 3 shows that alternated pumping results in a reduction of the salt intrusion length with 4 kilometres. The table and graph also show that salt intrusion length corresponding to alternated pumping is the same as the salt intrusion length of the steady state of a river discharge of 20 m³/s (no extractions). This effect already occurs after 1 day of alternated pumping.

Table 3: salt intrusion lengths corresponding to the curves in figure 10

Salt intrusion curve	Extraction rate [m ³ /s]	Volume extracted [m ³ /d]	Salt intrusion length (TA) [km]
Steady state Q=5 m ³ /s	15	1296000	76
Steady state Q=12.5 m ³ /s	7.5	648000	70
Steady state Q=20 m ³ /s	0	0	66
All curves with alternated pumping	0 or 15	648000	67

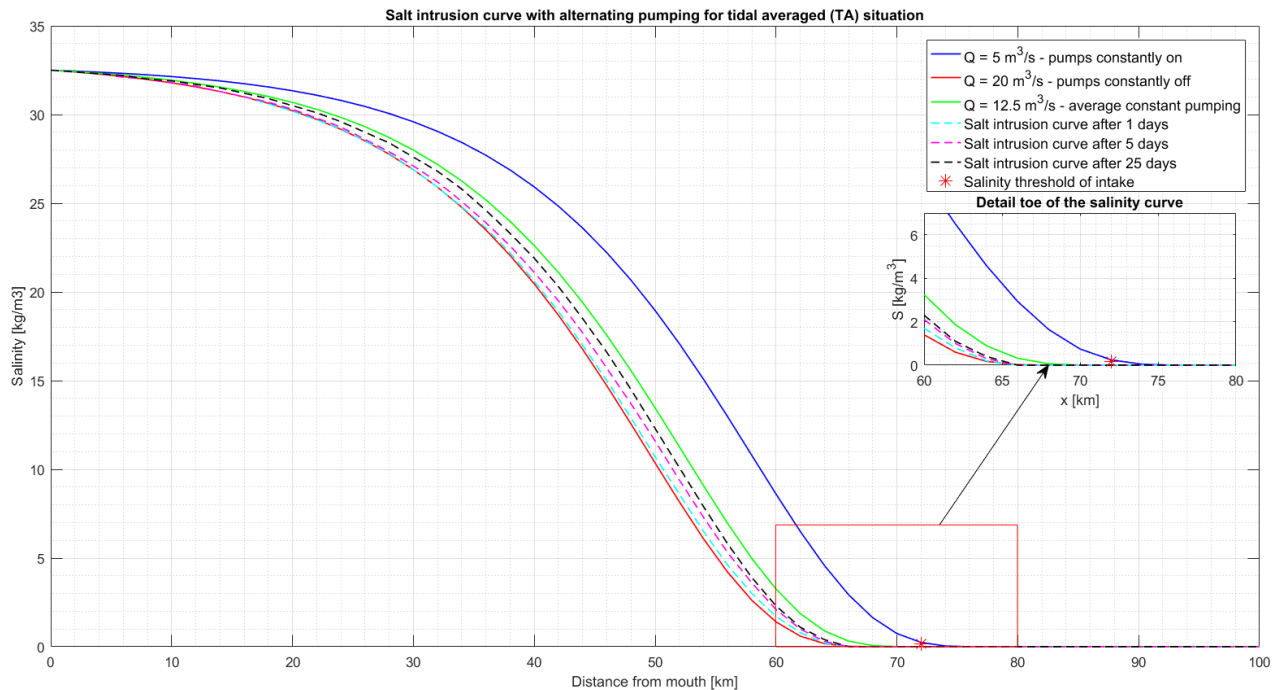


Figure 10: unsteady state simulation showing the salt intrusion curve in case of alternated pumping

5. Development of scenarios

In this chapter different scenarios will be developed to see the effects of extreme situations of the tide and river discharge on the salinity distribution in the Pungue estuary. For this analysis the steady state model is used, which is calibrated in the previous chapter. This model is representative if the changes in discharge and/or extraction rate are gradually. This assumption holds for the scenarios presented in this chapter.

5.1 Set up of the scenarios

The influence of the tide and the influence of the river discharge are the two most important drivers of salt intrusion in an estuary. In this chapter it is assumed that the salt intrusion is at its maximum during springtide and that the tidal range between different springtides will not vary significantly. Therefore a constant tidal range measured during springtide (December 2016) is applied to all scenarios and only the river discharge will be modified per scenario. The height of this tidal range is 5.8 meter. The parameters, which are used for the scenarios, are summarized in table 4. These parameters are determined in chapter 4.

Table 4: input parameters for steady state model scenarios

Parameter	H ₀ [m]	E ₀ [km]	K [-]	D ₀ [m ² /s]	S ₀ [kg/m ³]	h ₀ [m]	a [m]	A ₀ [m ²]
steady state model	5.8	20	0.2	calibrated formula	32.5	5.1	12255	36271

In order to come up with different scenario's more assumptions are needed regarding the extraction rate of Mafambisse, salinity threshold of the intake and extreme discharges. If the salt concentration at the intake exceeds 0.16 kg/m³ no water will be taken in and the pumps will be turned off. If the value exceeds this threshold the yield of the sugarcane will be seriously affected and the salt will damage the machines in the sugarcane factory. The management of the sugarcane estate sets this norm.

The intake of Mafambisse consists of eight mounted pumps and four additional pumps installed on a floating platform. Each pump has a capacity of about 1 m³/s. Under normal conditions there are four to eight pumps in operation. The remaining pumps are taken out for maintenance or function as backup. On average it can be assumed that six pumps are turned on resulting in an extraction rate of circa 6 m³/s.

Another issue which needs to be taken into account is the minimum water level needed at the intake. The pumps at the intake of the estate need a certain level to operate otherwise cavitation will occur, which can cause a lot of damage. Technical drawings of the pumps show that a minimum water level of 1.3 meter is needed for proper operation of the pumps. In order to translate this water level into a minimum river discharge a rating curve at the intake is needed, unfortunately this was not available during this research.

The intake of FIPAG is located 100 kilometres from the estuary mouth. This station provides drinking water for the city of Beira. The current extraction rate of FIPAG is around 1 m³/s (Levelt, van den Brink, & Dias, 2015).

To come up with extreme values for the river discharge a Gumbel analysis has been conducted on historical data of the discharge from the local water board ARA-Centro, measured at the station located next to the EN6 bridge over the Pungue. The dataset consist of a series of continuous recordings at Mafambisse from 1956 – 2004 (see Appendix B). The result of the Gumbel analysis and the corresponding return periods can be seen in the following table:

Table 5: results of the Gumbel analysis

Return period [years]	5	10	15	20
Discharge [m^3/s]	16	9	5	3

Before different scenarios will be evaluated the reference situation will be analysed. Afterwards the reference situation will be compared to the other scenarios. The other four scenarios are: expansion of the intake of FIPAG, increased extraction rate of the estate, a drought and a bend cutoff.

For each scenario a salt intrusion curve will be plotted. From this plot the maximum salt intrusion length (L) and the maximum salt concentration at the intake of the estate will be determined, both during high water slack (HWS) situation. The salt intrusion length is defined as the length from the mouth until the location where the salt concentration has decreased to the salinity of the river (0.01 kg/m^3). So it is possible that the salt intrusion length is equal or larger than the distance to the intake but the threshold of 0.16 kg/m^3 at the intake is not exceeded, this means that the pumps can stay on.

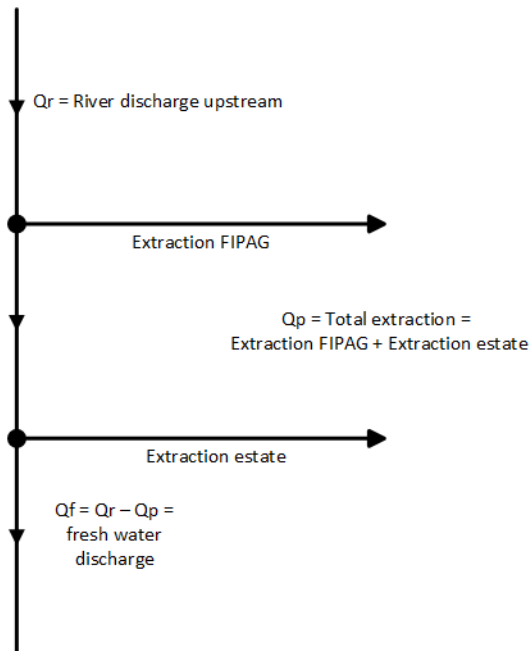


Figure 11: extraction scheme

5.2 Scenario 0: reference situation

For scenario zero a river discharge of $16 \text{ m}^3/\text{s}$ is chosen, this value can be seen as a representative value of the river discharge during a dry season, which has a return period of five years (see table 5). This value is without extractions or in other words it represents the river discharge upstream of the intake of FIPAG, see figure 11. With the average extraction of $6 \text{ m}^3/\text{s}$ of the estate and the extraction of $1 \text{ m}^3/\text{s}$ of FIPAG the discharge downstream of the intake of the estate becomes $9 \text{ m}^3/\text{s}$. As can be seen from the figure below during HWS (most extreme situation) the salt intrusion length is 78 km and the salinity threshold at the intake is not reached. This means that the estate can continuously extract a volume of $6 \text{ m}^3/\text{s}$ of water from the Pungue in this scenario.

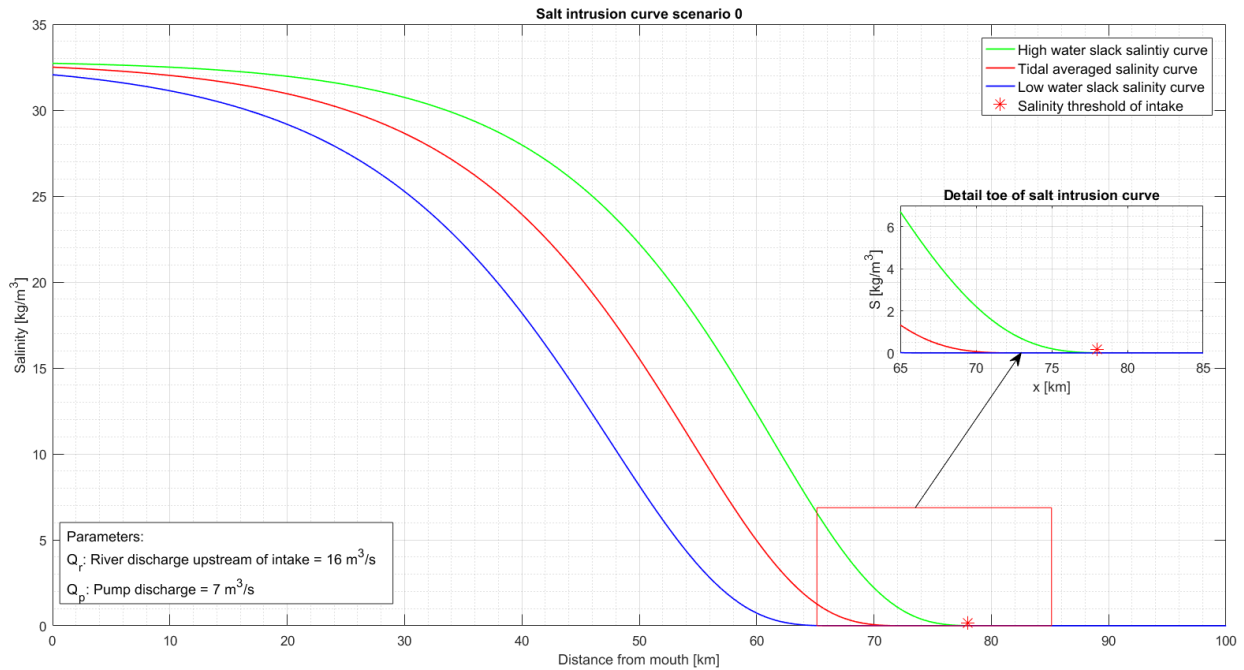


Figure 12: steady state simulation of the salt intrusion curve for the reference scenario

Table 6: results of the reference scenario

Scenario	Q_r [m^3/s]	Q_p [m^3/s]	$Q_r - Q_p$ [m^3/s]	L [km]	$S_{\text{max_intake}}$ [kg/m^3]
Reference scenario	16	7	9	78	0.00

5.3 Scenario 1: expansion of the intake of FIPAG

The city of Beira is developing rapidly, it is expected that the population of Beira will grow fast in the future (van Weelden, 2013). To provide enough drinking water to Beira with respect to the future, FIPAG needs to extract more water from the Pungue river. In the report: “Scoping study for the Beira drinking water supply in 2035” it is estimated that the extraction rate needs to be increased from the current 1 m³/s up to 2 m³/s in 2060. This is based on the growth of population from 577.771 people in 2014 to 1.936.660 people in 2060.

In this scenario the same upstream discharge of 16 m³/s is taken, this is the discharge without any extractions from FIPAG and the estate. If the extraction rate increases from 1 m³/s to 2 m³/s this will mean that the discharge upstream of the intake of the estate decreases to 14 m³/s. In this scenario it is assumed that the estate extracts on average 6 m³/s, this means that the fresh water discharge downstream of the intake becomes 8 m³/s.

This situation is plotted in the following figure and leads to a maximum salt intrusion length during HWS of 78 km. The maximum salt concentration at the intake does not exceed the threshold of 0.16 kg/m³, this means the pumps can stay on over the full tidal cycle.

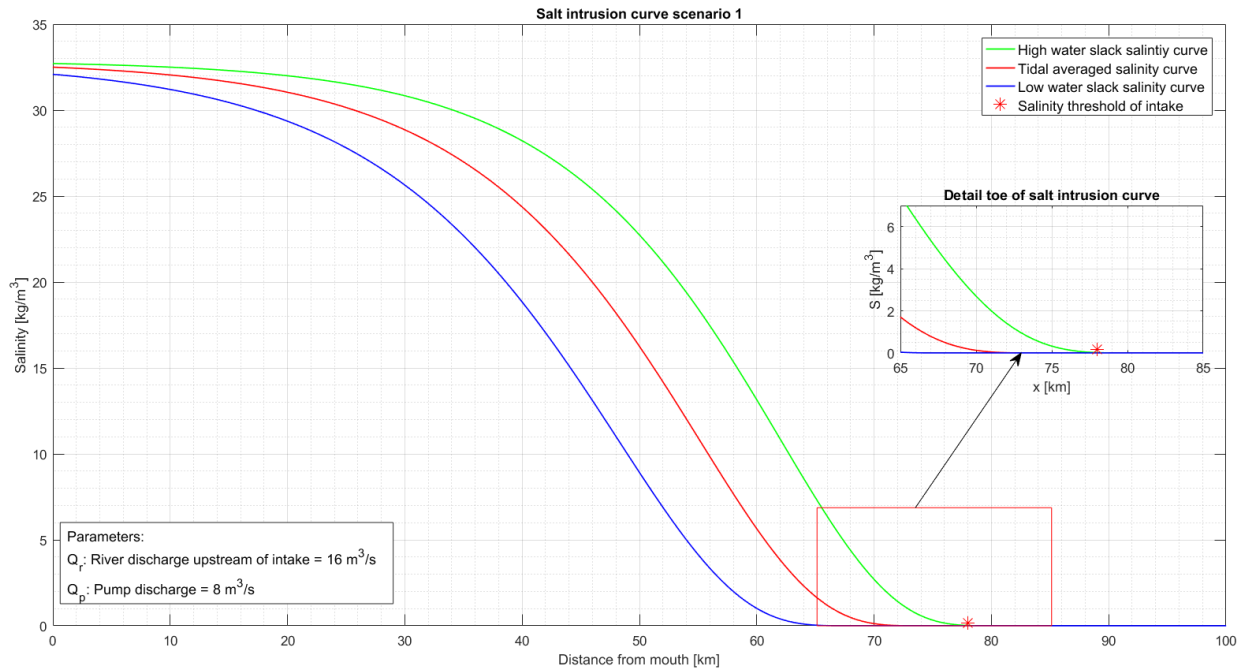


Figure 13: steady state simulation of the salt intrusion curve for scenario 1

Table 7: results of scenario 1

Scenario	Q_r [m ³ /s]	Q_p [m ³ /s]	$Q_r - Q_p$ [m ³ /s]	L [km]	S_{max_intake} [kg/m ³]
Expansion FIPAG	16	8	8	78	0.01

5.4 Scenario 2: increased extraction rate of the estate

Until now an average extraction rate of $6 \text{ m}^3/\text{s}$ is used. But the estate has the capacity to extract more water from the Pungue. There are some reasons why the water demand of the estate can increase:

- To maximize the yield of the sugarcane it can be necessary to increase the irrigation, so this will mean that also the extraction rate from the Pungue has to be increased.
- If there is a lack of precipitation at the estate for a long period but enough river discharge due to sufficient precipitation more upstream in Mozambique or Zimbabwe.
- In the future it is also possible that the estate will decide to expand.
- At the moment there are many unused plots. The estate is planning to cultivate these plots again. This will mean that the total area of sugarcane will increase from 6725 hectares to 7454 hectares (Moyo, 2016).

In this scenario the same upstream discharge of $16 \text{ m}^3/\text{s}$ with a return period of five years is taken. The extraction rate of the sugarcane estate is increased from $6 \text{ m}^3/\text{s}$ to $10 \text{ m}^3/\text{s}$ because of a higher water demand. This means that there are 10 pumps in operation and 2 pumps will be in maintenance or function as backup. It will always be necessary to have some pumps as backup in case of technical failure or maintenance. In this scenario the extraction rate of FIPAG is the same as in the reference scenario ($1 \text{ m}^3/\text{s}$), this means that the discharge downstream of the estate will be $5 \text{ m}^3/\text{s}$.

This situation is plotted in the following figure. As can be seen from the graph this leads to a maximum salt intrusion length of 81 km (HWS conditions). The maximum salt concentration at the intake is 0.24 kg/m^3 in this scenario, this is higher than the threshold so the pumps should be turned off around high water slack when the salt concentration is at its maximum.

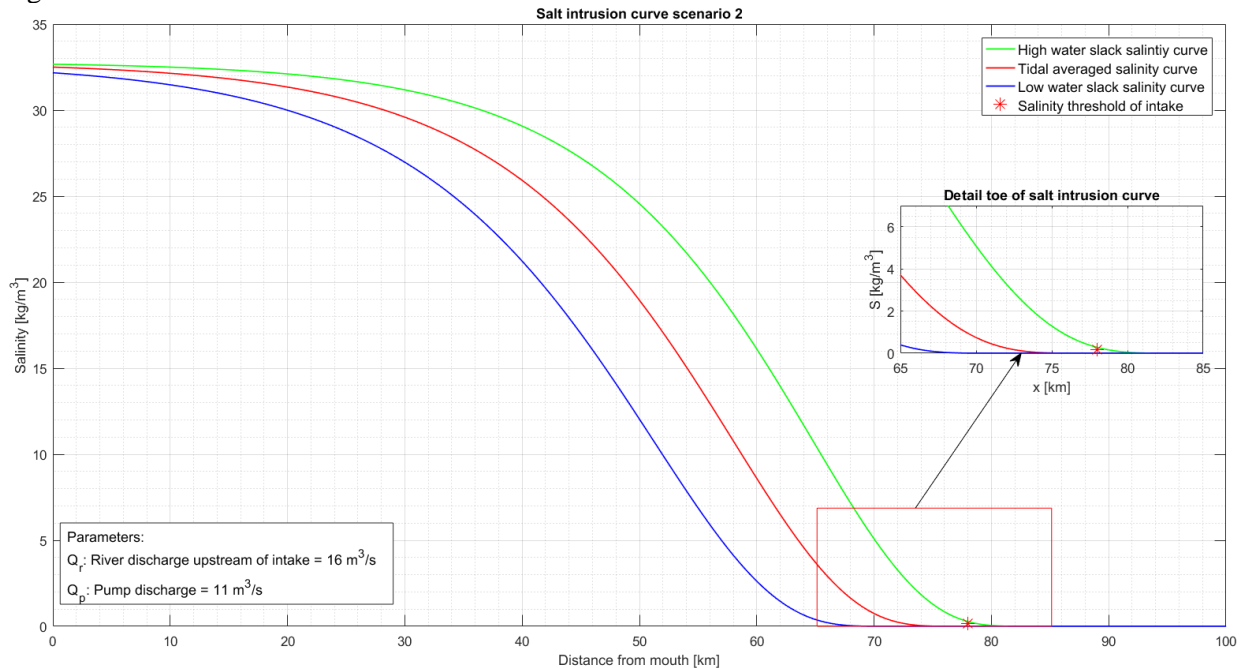


Figure 14: steady state simulation of the salt intrusion curve for scenario 2

Table 8: results of scenario 2

Scenario	Q_r [m^3/s]	Q_p [m^3/s]	$Q_r - Q_p$ [m^3/s]	L [km]	$S_{\text{max_intake}}$ [kg/m^3]
Increased extraction rate of the estate	16	11	5	81	0.24

5.5 Scenario 3: a drought

As can be seen from the Gumbel analysis of historical data big droughts have occurred in history and can occur again in the future. Due to climate change it is likely they will occur more frequently in the future. As stated in the introduction the Pungue river originates in Zimbabwe and a substantial amount (28 %) of the discharge is generated here (SWECO & Associates, 2004). When there is a big drought in Zimbabwe this also affects the river discharge up to Mafambisse.

The heaviest drought found in the Gumbel analysis is an upstream discharge of $3 \text{ m}^3/\text{s}$. This discharge has a return period of 20 years. With this river discharge it is impossible for the estate to extract enough water, because after the extraction of FIPAG of $1 \text{ m}^3/\text{s}$ only $2 \text{ m}^3/\text{s}$ is just upstream of the estate. Next to this the water level will probably be too low to extract water during low water and during high water the salt concentration certainly exceeds the threshold of the intake. So this value of the Gumbel analysis is not very interested to investigate any further because in this case the discharge is the limiting factor instead of the salinity.

It is interested to investigate the situation in which the upstream discharge is $9 \text{ m}^3/\text{s}$ with a corresponding return period of 10 years. If the estate extracts the average capacity of $6 \text{ m}^3/\text{s}$ from the Pungue and FIPAG $1 \text{ m}^3/\text{s}$ the remaining discharge will be $2 \text{ m}^3/\text{s}$. This scenario is plotted in figure 15 with the steady state model.

As can be seen from the graph the salt intrusion length during HWS (most extreme situation) in this scenario is around 84.5 km and the maximum salt concentration at the intake is 2.63 kg/m^3 at HWS and on average 0.18 kg/m^3 . This means that the estate has to shut off their pumps for most of the time in this scenario.

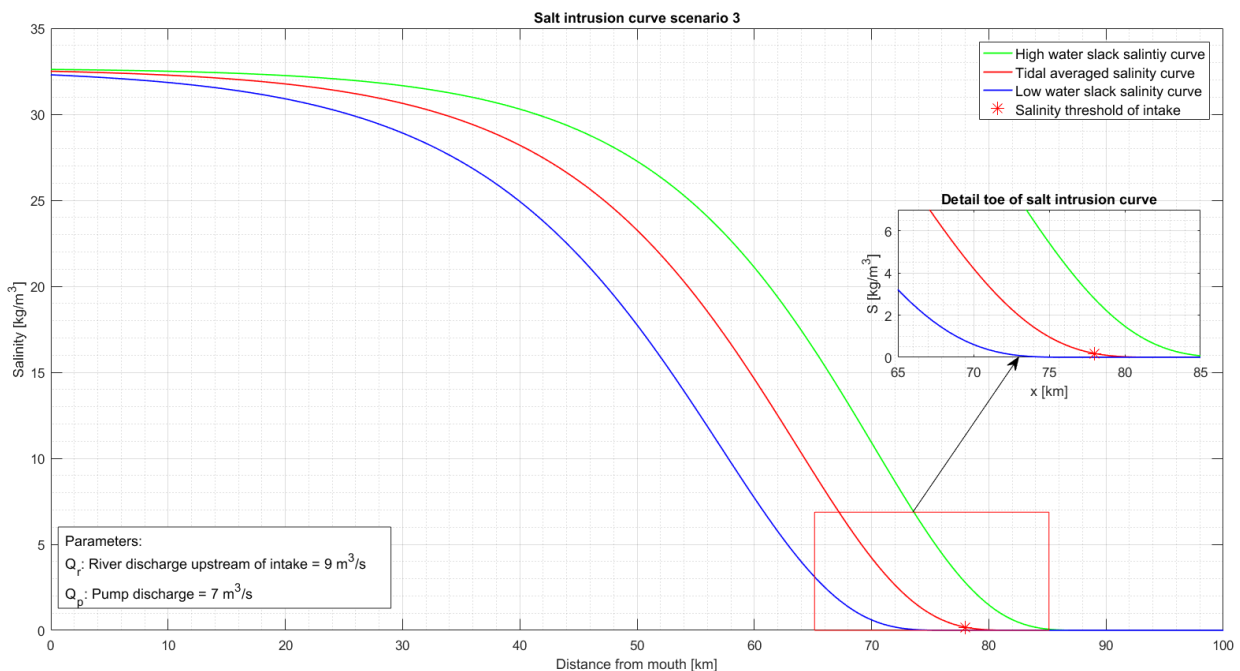


Figure 15: steady state simulation of the salt intrusion curve for scenario 3

Table 9: results of scenario 3

Scenario	Q_r [m ³ /s]	Q_p [m ³ /s]	$Q_r - Q_p$ [m ³ /s]	L [km]	S_{\max_intake} [kg/m ³]
A drought	9	7	2	84.5	2.63

5.6 Scenario 4: bend cutoff

The Pungue river is very dynamic due to its natural behaviour. This results in a lot of erosion and sedimentation. Only on the side of the estate the riverbank is fixed by a dike, the other bank consist out of natural vegetation and forms a natural levee. In 2009 the last two bend cutoffs occurred, this shortened the river by approximately 10 kilometres (measured from historical Google Earth images).

There are some other bends, which have moved a lot the past decade. It is possible that one of these bends will cutoff in the future (see figure 16). Deltares has developed an open source application the Aquamonitor (Donchyts et al., 2016) that compares historical satellite images of rivers with the latest available images. The application shows the sedimentation and erosion, which has happened over the past 15 years. In figure 16 a screenshot of the possible bend cut offs in the Pungue estuary are shown. The green areas represent the sedimentation and the blue areas the erosion from 2000 until 2016. When analysing this picture it becomes clear that two bends are growing to each other, it is possible that these will cut off in the future.



Figure 16: screenshot Aquamonitor of possible bend cutoffs. Green = sedimentation, blue = erosion (Donchyts et al., 2016)

From Google Earth images it is measured that a bend cutoff will lead to a shortening of approximately 6 kilometres of the river. Both bends are approximately of the same size. As can be seen in figure 16 only one of the bends will cutoff. The water will follow another path once this has occurred making it impossible to cutoff the other bend as well. These bends are located downstream of the Mafambisse water intake. A bend cut off will mean that the location of the water intake will be relatively six kilometres closer to the sea (not taken into account that the river bends are also growing slowly over time).

In figure 17 the salt intrusion curves are plotted with the same discharge as in the reference scenario. But in this figure the threshold/location of the intake of the estate is moved six kilometres closer to the mouth. The corresponding maximum salt intrusion length stays the same as the reference scenario (78 kilometres) but with the new location of the intake the salinity threshold is exceeded. The salt concentration at the intake has increased from 0.0036 kg/m^3 to 1.10 kg/m^3 , this means that the pumps have to be shut off.

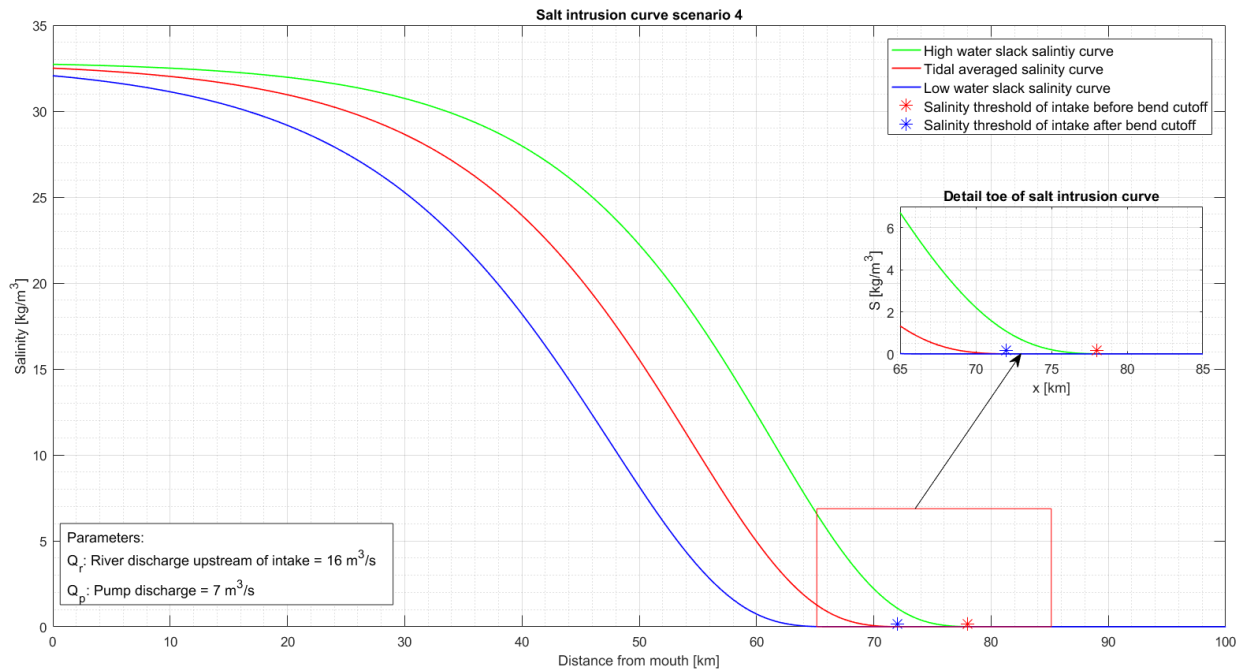


Figure 17: steady state simulation of the salt intrusion curve for scenario 4

Table 10: results of scenario 4

Scenario	Q_r [m^3/s]	Q_p [m^3/s]	$Q_r - Q_p$ [m^3/s]	L [km]	$S_{\text{max_intake}}$ [kg/m^3]
Bend cut off	16	7	9	78	1.10

5.7 Summary of the scenarios

In table 11 all results of the scenarios are summarized. This table shows the effect of the different measures in terms of maximum salt intrusion length (L) and maximum salt concentrations at the intake (S_{\max_intake}), which occur during high water slack (HWS) conditions. The return periods indicate the probability that the corresponding upstream discharge (Q_r) occurs and the timescale of the measures give an indication when the changes in extraction rates or the bend cutoff can be expected.

Scenario 1 does not lead to a critical scenario but it is certain that FIPAG will expand its capacity before 2060, after this expansion the discharge will decrease with $2 \text{ m}^3/\text{s}$ instead of $1 \text{ m}^3/\text{s}$ at all other scenarios.

Scenario 2, 3 and 4 all lead to a maximum salt concentration (during HWS) which is higher than the threshold of the intake. Scenario 3 also results in an average salt concentration, which exceeds the threshold of $0.16 \text{ kg}/\text{m}^3$.

It is also possible that the river discharge will decrease due to extractions or changes in the river more upstream in Mozambique or Zimbabwe. In this report these scenarios are not taken into account because this is beyond the scope of this research.

Table 11: summary of the outcome of the different scenarios

Scenario	Q_r [m^3/s]	Q_p [m^3/s]	$Q_r - Q_p$ [m^3/s]	Return period of Q_r [years]	Timescale measures	L [km]	S_{\max_intake} [kg/m^3]
0. Reference scenario	16	7	9	5	-	78	0.00
1. Expansion FIPAG	16	8	8	5	Short term	78	0.01
2. Increased extraction rate Mafambisse	16	11	5	5	Unknown	81	0.24
3. A drought	9	7	2	10	-	84.5	2.63
4. Bend cut off	16	7	9	5	Long term	78	1.10

6. Conclusions and recommendations

6.1 Conclusions

The first conclusion, which can be drawn, is that the geometry of the Pungue estuary can be well described exponentially. Both the width and the cross-sectional area obey the characteristics of an exponential function. As mentioned in chapter 4 the geometry can be well modelled in one branch, because no significant inflection points are visible if one would plot the width and cross-sectional area on semi logarithmic paper. The convergence lengths for respectively width and cross-sectional convergence can be determined from the slopes of the exponential trend lines.

Another conclusion made is that the steady state model is unable to represent the sudden increase in salinity values conducted by the moving-boat method on the 15th, 16th and 17th of December 2016. Despite the fact that the high-salinity values observed at the river section $x = 40$ km up to $x = 60$ km are badly represented by the steady state model it is a good indicator for the salt intrusion length. Also the fact that the toe of the salt intrusion curve is not affected by these high and local salinity values support this conclusion. It is likely that the saline water that remained after flooding of the right bank (West) by a storm surge was flushed out by intensive rain. A net rainfall event of 3.5 mm/d (responsible for the generation of runoff) would have been enough to generate this salt source.

It is likely that the irregularities observed in the salinity values are caused by an additional source of salt. The unsteady state model makes it possible to add an additional salt source and to include the effect of pumping (by Mafambisse and FIPAG). Once this additional salt source is included it is possible to approach high salinity values at the river section as observed during the measurement campaign.

Chapter 4.3.4 shows a simulation of an alternated pumping scheme. The salt intrusion length with this alternated pumping scheme is shorter than the salt intrusion length that corresponds to a constant extracting rate. This results in a river discharge of 12.5 m³/s. This means that with alternated pumping the toe of the salt intrusion curve is further from the intake, so it should be possible to extract more water in this situation in comparison to a situation with a constant extraction rate. This result is already achieved after one day of alternated pumping, after this period the toe of the salt intrusion curve reaches a steady state. The salt concentrations more downstream of the toe slightly increase over time but never reach the steady state of the constant extraction rate. This proves that in this extreme scenario alternated pumping can be beneficial for the estate.

From the scenarios it can be concluded that scenarios 2 (expansion Mafambisse), 3 (a drought) and 4 (bend cutoff) exceed the salinity threshold at the intake of 0.16 kg/m³, causing water shortages for irrigation and process purposes. From these three scenarios, which exceed the salinity threshold at the intake, scenario 3 (a drought) is the most extreme. The maximum modelled salinity value at the intake reaches 2.63 kg/m³. This scenario also leads to the highest salt intrusion length. The salt intrudes up to 84.5 km. In this situation no extractions are possible and Mafambisse will suffer from severe water shortages.

6.2 Recommendations

In this paragraph recommendations are provided on how the estate can reduce or prevent future salt incidents at the intake. The recommendations are divided into three categories: relocation of the intake, alternated pumping and monitoring of additional salt sources.

6.2.1 Relocation of the intake

A straightforward solution to reduce the salt incidents at the intake of Mafambisse would be the relocation of the pumping station. This new to be determined location should fulfil certain requirements of which the biggest requirement would be that it should be further located than the maximum modelled salt intrusion length. In other words it should be further upstream than 84.5 km from the estuary mouth as modelled in the most extreme scenario (scenario 3: a drought). To incorporate the effect of a possible bend cutoff or the fact that the steady state model is just an indicator for salt intrusion this 84.5 km needs to be corrected with a safety margin. The value of the safety margin is arbitrary, but if a bend cutoff would occur this would mean that there is a relative shift around 6 km on the estuary x -axis. Therefore if one would have to choose a safe location this research recommends building a new pumping station at 90 km or further from the estuary mouth.

6.2.2 Alternated pumping

This research shows that alternated pumping can be beneficially in situations with a large salt intrusion length. This occurs when the river discharge is low during spring tide. In this situation the estate extract a significant part of the fresh water discharge, this makes it possible to flush the salt downstream when turning off the pumps. Most of the time it will not be necessary to apply alternated pumping at the intake of the estate, because the salt concentrations with continuously pumping stay below the salinity threshold of the intake.

Another remark, which has to be made, is that the estate currently automatically applies his own version of alternated pumping. When the discharge is low during spring tide the pumps are switched off around high water slack because the salt concentrations at the intake are too high. Sometimes the pumps are also switched off during some hours around low water because the water level is too low. This behaviour also leads to a form of alternated pumping.

It will be more efficient when the estate uses an alternated pumping scheme before the salt reaches the intake. In this way it is possible to have influence on the salt intrusion length before you have to stop extracting water because the salt concentrations have become too high at the intake. At the moment this will be hard to realize because the estate does not have any regular measurements of the upstream discharge and does not have regular measurements of the salt concentrations more downstream. Without this information it is very hard to predict the salt intrusion length only based on tide tables and regular salinity measurements at the intake.

6.2.3 Monitoring an additional salt source

As mentioned in the conclusion it is likely that the measured increase in salinity during the measurement campaign is caused by an additional source of salt. In this particular case the increase of salinity values at the river section $x = 40$ km up to $x = 60$ km does not affect the toe of the salt intrusion curve. In other words the salt concentrations at the intake are not affected by this local increase, but this does not imply this will be the case in the future. Therefore it is interesting to monitor additional salt sources because this can result in salt incidents at the intake. The authors suggest the following recommendations:

- Monitor the salinity of the water in the main drainage channel. If this is too high you can place sluices between the drainage channels of the unused plots and the main drainage channel. With this sluices the estate can control the drainage of saline water. This water can be drained to the river when it is neap tide or if the river discharge is high. When the salt intrusion is big these sluices will prevent that extra salt is added to the river.
- Investigate the flood plain next to the river section 60 km from the estuary mouth. If this is a place where river water enters the floodplain during a flood event and is stored for some time the water will partly evaporate and the remaining part will be highly saline. This water can be flushed into the river during a rain event causing high local salinity values. To prevent the water from entering the floodplain one could think of the following solutions. The first measure would be to place sluices, which prevent the water flowing into this flood plain. It also works the other way around, because it also prevents that water from the floodplain flows back into the river. A second rather straightforward solution would be to increase the natural levee at the side of the riverbank, to prevent flooding.

7. Further research

In this chapter some aspects of this research are discussed which are interesting for follow up research. Next to this the authors suggest some other topics, which are beyond the scope of this research but are interesting to investigate.

The following topics are interesting for follow up research:

- **More salinity measurements between $x = 60$ km and $x = 78$ km:**
In this research it was not possible to conduct salinity measurements between 60 kilometres and 78 kilometres (intake of the estate). This was the case because during the measurement campaign we started from the mouth of the estuary and we had to return before low water makes it impossible to navigate. Also the amount of sun hours was limited, which forced us to return early and made it impossible to measure between 60 km and 78 km. A solution to this would be to make use of two different boats. For the first 40 km one would need a big boat with sufficient horsepower, while the estuary is quite wide and there are some deep channels. For the second part of the estuary, where it is more shallow and narrow, one would need a smaller boat but it should have enough horsepower to catch up with the tidal wave.
- **Measure over a longer period:**
The measurement results in this research are collected during one week. It was not possible to collect more measurements due to the limited duration of the stay and practical problems like engine failure and the availability of suitable boats. A longer measurement period will result in a better calibration of the steady and unsteady state salt intrusion model.
- **Install more divers:**
Due to stolen divers and engine problems it was only possible to install and collect four CTD divers during this research. It is very hard to install the equipment on a safe/invisible place and without a good boat it is nearly impossible to install the equipment. To make a good comparison between the measurements of the CTD divers and the measurements conducted with the moving-boat method more divers need to be installed.
- **Monitor additional salt source:**
In chapter 4 an additional salt source is described. In this research there was not sufficient time to investigate the origin of this source. In the future students/researchers can identify the additional salt source by conducting salinity measurements at the drainage channel, the unused plots and at the flood plain next to the river.
- **Pump operation control depending on real time monitoring of salinity and river discharge:**
To see what the effect of alternated pumping would be in practice one needs to develop an alternated pumping scheme and test this in reality. Before this could be applied it is advised to come up with some theoretical scenarios and further investigate the phenomenon of alternated pumping. Furthermore to investigate a strategy for alternated pumping one need to monitor the salinity values downstream of the intake and the river discharge upstream of the intake in real time. By doing this it is possible to predict and model the effect on the salt intrusion curve. The user can adapt their extraction scheme depending on this model and the real time salinity and discharge measurements.

Other topics, which can be interesting to investigate:

- **Development of bend cutoffs:**
It will be interesting to determine the speed of this process and the sediment fluxes in the river.
- **Occurrence of a tidal bore:**
Literature and the result of the CTD diver next to the intake give indications that a tidal bore occurs in the Pungue. This phenomenon can be a topic for further research.
- **Effects of dredging at the port of Beira:**
In Beira there is a navigation channel to the port, which is located in the mouth of the river. The effects of this dredged navigation channel on the salt intrusion can be an interesting topic for further research.
- **Influence of upstream interventions in the river:**
Human actions such as extractions or the construction of a dam upstream in Mozambique or Zimbabwe can have a big influence on the river discharge. This will lead to an increase of the salt intrusion length.

References

- Dionne, J. C. (1963). Towards a more adequate definition of the St. Lawrence estuary. *Zeitschrift fur Geomorphologie*, 7, 36-44.
- Donchyts, G., Baart, F., Winsemius, H., Gorelick, N., Kwadijk, J., & van de Giesen, N. (2016). Earth's surface water change over the past 30 years. *Nature Climate Change*, 6(9), 810-813.
- Fischer, H. (1972). Mass transport mechanisms in partially stratified estuaries. *Journal of fluid mechanics*, 53(04), 671-687.
- Flater, D. (1998). Mobile Geographics LLC. Retrieved from <http://tides.mobilegeographics.com/locations/483.html>.
- GoogleEarth. (2016). Google Earth Imagery.
- Graas, S. (2002). *Improved model for the salt intrusion in the pungoe estuary*. Retrieved from Beira, Mozambique.
- Hegnauer, M., & Savenije, H. H. G. (2009). Salt intrusion in the Pungue estuary: Unsteady state situation because of upstream pumping.
- Levelt, L., van den Brink, R., & Dias, S. (2015). *Scoping Study for the Beira drinking water supply in 2035*. Retrieved from Utrecht, The Netherlands.
- Moyo, C. (2016) *Increased extraction rate of the estate/Interviewer: I. Abas & H. P. Hagedooren*.
- Sanders, B. F., & Piasecki, M. (2002). Mitigation of salinity intrusion in well-mixed estuaries by optimization of freshwater diversion rates. *Journal of Hydraulic Engineering*, 128(1), 64-77.
- Savenije, H. H. G. (1986). A one-dimensional model for salinity intrusion in alluvial estuaries. *Journal of Hydrology*, 85(1-2), 87-109.
- Savenije, H. H. G. (1988). Influence of rain and evaporation on salt intrusion in estuaries. *Journal of Hydraulic Engineering*, 114(12), 1509-1524.
- Savenije, H. H. G. (1989). Salt intrusion model for high-water slack, low-water slack, and mean tide on spread sheet. *Journal of Hydrology*, 107(1-4), 9-18.
- Savenije, H. H. G. (1992b). Rapid assessment technique for salt intrusion in alluvial estuaries.
- Savenije, H. H. G. (1993). Predictive model for salt intrusion in estuaries. *Journal of Hydrology*, 148(1), 203-218.
- Savenije, H. H. G. (2006). *Hydrology of Catchments, Rivers and Delta's*. Delft, The Netherlands: University of Technology Delft.
- Savenije, H. H. G. (2012). *Salinity and Tides in Alluvial Estuaries*. New York: Delft University of Technology.
- Savenije, H. H. G., & Pagès, J. (1992a). Hypersalinity: a dramatic change in the hydrology of Sahelian estuaries. *Journal of Hydrology*, 135(1-4), 157-174.
- SWECO, & Associates. (2004). *The Pungwe River Monograph Main Report*.
- Terink, W., & Droogers, P. (2014). *Hydrological analysis and modelling of the Pungwe River Basin, Mozambique*. Retrieved from Wageningen, The Netherlands.
- van Weelden, P. (2013). *Masterplan Beira Mozambique*. Retrieved from Delft, The Netherlands:
- Zanting, H. A., Macueve, C., & Novela, B. (1994). *Salt intrusion in the pungue estuary*. Retrieved from Maputo, Mozambique.

List of figures

Figure 1: overview of the Pungue estuary and relevant locations	9
Figure 3: definition salt intrusion curve and plotted LWS, TA and HWS situation.....	14
Figure 4: locations of the installed divers	21
Figure 5: corrected widths, depths and cross-sectional areas for tidal average situation	23
Figure 6: steady state simulation and moving-boat measurements on the 15 th , 16 th and 17 th	24
Figure 7: detail of river section with irregular salt distribution between $x = 40$ km to $x = 60$ km from	26
Figure 8: historical images of river section where salt is added $x = 40$ km to $x = 60$ km from.	27
Figure 9: unsteady state simulation with additional salt source for TA situation	29
Figure 10: unsteady state simulation showing the salt intrusion curve in case of alternated pumping	31
Figure 11: extraction scheme	33
Figure 12: steady state simulation of the salt intrusion curve for the reference scenario	34
Figure 13: steady state simulation of the salt intrusion curve for scenario 1	35
Figure 14: steady state simulation of the salt intrusion curve for scenario 2	36
Figure 15: steady state simulation of the salt intrusion curve for scenario 3	37
Figure 16: screenshot Aquamonitor of possible bend cutoffs. Green = sedimentation,	38
Figure 17: steady state simulation of the salt intrusion curve for scenario 4	39
Figure 18: definition sketch of geometry parameters	48
Figure 19: Gumbel analysis	51

List of tables

Table 1: geometry parameters.....	22
Table 2: values of the calibration parameters for the steady state model	24
Table 3: salt intrusion lengths corresponding to the curves in figure 10	31
Table 4: input parameters for steady state model scenarios.....	32
Table 5: results of the Gumbel analysis.....	33
Table 6: results of the reference scenario	34
Table 7: results of scenario 1	35
Table 8: results of scenario 2	36
Table 9: results of scenario 3	37
Table 10: results of scenario 4	39
Table 11: summary of the outcome of the different scenarios	40
Table 12: measured and corrected cross-sections, from $x = 0$ km to $x = 35$ km.....	48
Table 13: measured and corrected cross-sections, from $x = 36$ km to $x = 100$ km	49
Table 14: discharges with corresponding return periods taken from figure 19.....	51

Appendix A: determination geometry parameters

In this appendix the measured cross-sections and geometry data are given which are used to determine the geometry parameters in chapter 4.1. Table 12 shows the measurements of the cross-sections and figure 18 shows a definition sketch of the parameters. The values indicated with * are depth measurements from the report of Graas (2002).

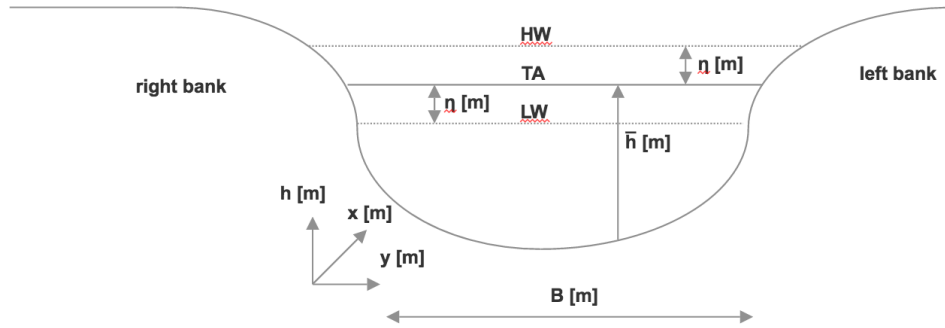


Figure 18: definition sketch of geometry parameters

Table 12: measured and corrected cross-sections, from $x = 0$ km to $x = 35$ km

x [m]	B [m]	$B - B_r$ [m]	h_{obs} [m]	η [m]	h_{TA} [m]	A_{obs} [m ²]	A [m ²]	$A - A_r$ [m ²]
0	7184	7154	4.57	-0.50	5.07	32831	36423	36271
2500	5960	5930						
2930	6310	6280	4.67	-0.25	4.92	29468	31028	30880
5000	7211	7181						
7500	4528	4498						
10000	3970	3940						
12500	3380	3350						
15000	2872	2842						
17500	2124	2094						
20000	2949	2919						
21780	2170	2140	3.90	0.58	3.32	8463	7214	7114
22500	3200	3170						
25000	2191	2161						
26438	1418	1388	5.62	0.81	4.81	7969	6814	6670
27500	1260	1230						
29720	1005	975	4.60	0.94	3.66	4623	3680	3570
30000	1010	980						
32500	984	954						
33870	655	625	5.89	0.92	4.97	3858	3253	3104
35000	1109	1079						

Table 13: measured and corrected cross-sections, from $x = 36$ km to $x = 100$ km

x [m]	B [m]	$B - B_r$ [m]	h_{obs} [m]	η [m]	h_{TA} [m]	A_{obs} [m ²]	A [m ²]	$A - A_r$ [m ²]
36137	737	707	4.46	0.92	3.54	3287	2612	2506
37500	1095	1065						
40000	1118	1088						
42500	618	588						
45000	507	477						
47500	448	418						
50000	288	258						
52500	293	263						
55000	238	208						
57500	244	214						
60000	145	115			2.63*		381	302
60600	113	83	1.90	-0.10	2.00	215	226	166
62000	170	140			2.73*		464	382
62500	100	70						
65000	120	90			2.68*		321	241
67000	90	60			3.01*		271	181
67500	66	36						
70000	90	60			2.90*		261	174
72500	64	34						
75000	55	25						
77000	65	35			3.05*		198	107
77500	58	28						
79000	57	27			2.40*		137	65
80000	57	27						
81000	43	13			2.75*		118	36
82500	54	24						
84561	46	16	2.44	-0.47	2.91	112	134	47
85000	40	10						
87500	42	12						
90000	41	11						
92500	44	14						
95000	43	13						
97500	47	17						
100000	41	11						

Appendix B: Gumbel extreme value distribution

This appendix contains a statistical analysis of minimum discharges of the hydrometric station located at Mafambisse. In order to calculate different return periods corresponding to different minimum discharges, continuous recordings at Mafambisse in the period 1956 – 2004 are analysed.

This analysis is done by making use of the Gumbel extreme value distribution theory, which is a method to distribute extreme values and is well known for its application in statistics but also it is often used to describe hydrological events.

B.1: Gumbel type I

The Gumbel extreme value distribution theory (Savenije, 2006) has been used widely in hydrology to describe different hydrological events. In short the fundamental theorem can be stated as follows:

If $X_1, X_2, X_3, X_4, \dots, X_n$ are independent extreme hydrological events, observed in a dataset of n samples of equal size N (e.g. years), and X is an unlimited exponentially distributed variable under the condition that n and N approach infinity, the cumulative probability q , which expresses the probability that any event is less than a given value X_i , is given by:

$$q = \exp(-\exp(-y)) \quad (\text{B.1})$$

Where q is the cumulative probability which will not be exceeded and y is the reduced variate. With the above definition also p can be calculated, where p is the cumulative probability that a certain event exceeds a given value X_i .

$$p = 1 - q \quad (\text{B.2})$$

The reduced variate y can be rewritten as follows:

$$y = -\ln(-\ln(1 - p)) = -\ln(-\ln(1 - \frac{1}{T})) \quad (\text{B.3})$$

Where T is a so called return period, which is calculated from the dataset of N years. The return period T expresses the probability that a certain event will occur within a given time period.

According to Gumbel the reduced variate y can be defined as a linear function:

$$y = a(-X - b) \quad (\text{B.4})$$

Where a is the so-called dispersion factor and b is the mode. Gumbel showed that if the sample is finite, which they always are, the coefficients a and b can be described by the following equations:

$$a = \frac{s_y}{s} \quad (\text{B.5})$$

$$b = X_m - \frac{y_m}{s_y} \quad (\text{B.6})$$

Where X_m is the mean of the extremes and s is the standard deviation of the sample. Furthermore s_y stands for the standard deviation of the set of reduced variables y . This equation can be modified to:

$$X = X_m - \frac{(y - y_m)s}{s_y} \quad (\text{B.7})$$

This equation only applies for minimum flow.

B.2: Log-Gumbel type III

The log-Gumbel type III distribution (Savenije, 2006) is often used for the analysis of extreme flows. In particular it can be used for the analysis of minimum flows. The probability that a certain value exceeds the minimum flow is given by the following formula of p :

$$p = 1 - \frac{i-0.25}{n+0.5} \quad (\text{B.8})$$

Where p represents a plotting position and i is the rank number of the extreme, in this case the rank number of the minimum flow. In the above formula n stands for the number of years observed. The reduced variate y of Gumbel can be computed by:

$$y = -\ln(-\ln(p)) \quad (\text{B.9})$$

Combining Log-Gumbel III with Gumbel type I distribution gives the following result:

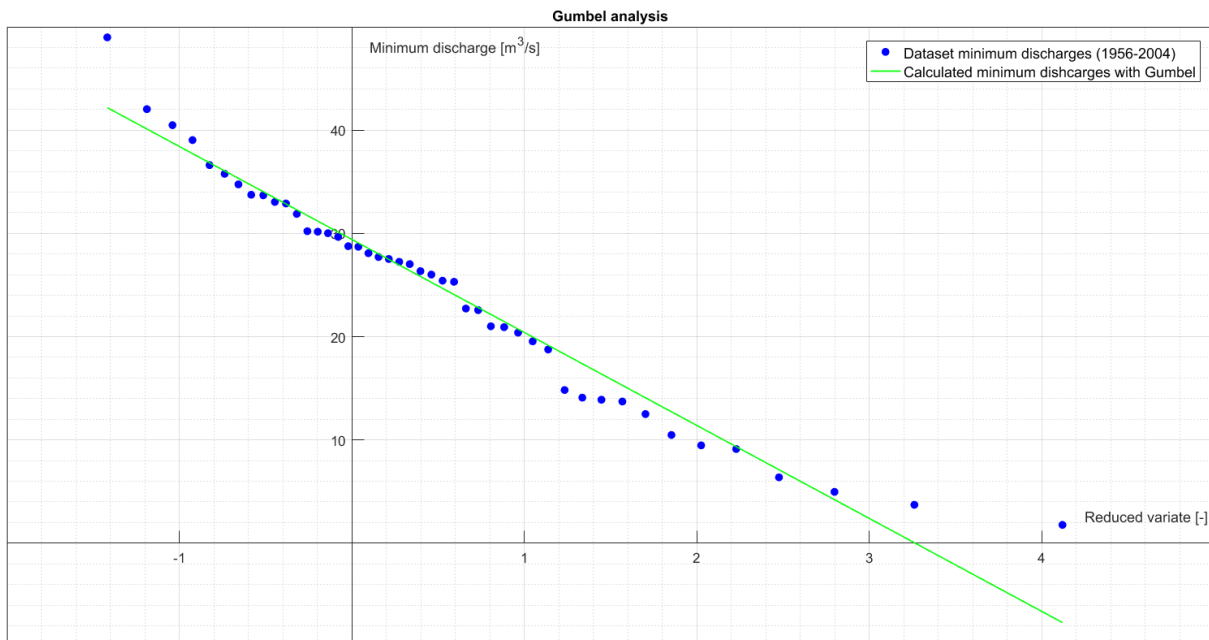


Figure 19: Gumbel analysis

From figure 19 in combination with formula B.3 the minimum discharges can be linked to corresponding return periods. The results are given in the following table:

Table 14: discharges with corresponding return periods taken from figure 19

Return period [years]	5	10	15	20
Discharge [m^3/s]	16	9	5	3

